JOURNAL OF SPACECRAFT AND ROCKETS
Vol. 61, No. 4, July–August 2024

General Dynamics for Single- and Dual-Axis Rotating Rigid Spacecraft Components

João Vaz Carneiro*
University of Colorado Boulder, Boulder, Colorado 80303
Cody Allard†
Laboratory for Atmospheric and Space Physics, Boulder, Colorado 80303
and
Hanspeter Schaub‡
University of Colorado Boulder, Boulder, Colorado 80303

https://doi.org/10.2514/1.A35865

Deriving and propagating a spacecraft's equations of motion is fundamental to describing its behavior accurately. These equations of motion depend on the spacecraft's configuration, which includes any physical subsystem such as attitude control devices, solar panels, gimbals, etc. Prior work introduced the backsubstitution method to yield a modular and scalable formulation to develop complex spacecraft dynamics specific to rotating components attached to a rigid hub as effectors. This paper relaxes assumptions made in deriving effector components in prior work, such as mass properties and frame definitions. This produces a general architecture that uses common equations of motion for physically equal parts. The result is an analytical solution of a set of general rotating effector equations of motion that greatly expand the configuration space of spacecraft that can be simulated with the backsubstitution method. In contrast to prior work where the rotations are highly constrained, rigid-body components can rotate about one or two general axes, and the component mass distribution can be general, no longer requiring the component's principal axis to align with the center of mass or hinge axis. A numerical software solution demonstrates and verifies how these effectors can mimic a range of dynamic spacecraft components.

Nomenclature

$\boldsymbol{A}_c$	=	center-of-mass location of body A
$\boldsymbol{a}_{ij}$	=	effector backsubstitution term for $\ddot{\boldsymbol{r}}_{B/N}$
$\dot{\boldsymbol{a}}$, $\ddot{\boldsymbol{a}}$	=	first- and second-order time derivatives of vector $\boldsymbol{a}$ with respect to the inertial frame $\mathcal{N}$
$\boldsymbol{a}'$, $\boldsymbol{a}''$	=	first- and second-order time derivatives of vector $\boldsymbol{a}$ with respect to the body frame $\mathcal{B}$
$[\tilde{\boldsymbol{a}}]$	=	cross-product operator written in matrix form
$\boldsymbol{b}_{ij}$	=	effector backsubstitution term for $\dot{\boldsymbol{\omega}}_{B/N}$
C	=	center-of-mass location of the system
$\boldsymbol{c}$	=	vector from point B to the center of mass of the spacecraft C, m
$\boldsymbol{c}_{ij}$	=	independent effector backsubstitution term
$\boldsymbol{F}_{\text{ext}}$	=	vector sum of external forces on the spacecraft, N
$[I_{A,A}]$	=	inertia tensor of body A with respect to point A, kg · m^2
$\boldsymbol{L}_B$	=	vector sum of external torques on the spacecraft about point B, N · m
m_A	=	mass of body A, kg
N, B, S	=	origin point for inertial, body, and component frames
$\mathcal{N}, \mathcal{B}, \mathcal{S}$	=	inertial, body, and component frames
$\boldsymbol{r}_{A/B}, \dot{\boldsymbol{r}}_{A/B}, \ddot{\boldsymbol{r}}_{A/B}$	=	linear position, m; inertial velocity, m/s; and inertial acceleration of point A with respect to B, m/s^2
u_S	=	scalar torque applied to the hinge, N · m
$\theta, \dot{\theta}, \ddot{\theta}$	=	hinge's angle, rad; angle rate, rad/s; and angle acceleration, rad/s^2
$\boldsymbol{\sigma}_{\mathcal{A}/\mathcal{B}}$	=	attitude of frame $\mathcal{A}$ with respect to frame $\mathcal{B}$ expressed in modified Rodrigues parameters
$\boldsymbol{\omega}_{\mathcal{A}/\mathcal{B}}, \dot{\boldsymbol{\omega}}_{\mathcal{A}/\mathcal{B}}$	=	angular velocity, rad/s, and inertial acceleration of frame $\mathcal{A}$ with respect to $\mathcal{B}$, rad/s^2

Subscripts

i	=	ith component body
hub	=	spacecraft's hub
sc	=	spacecraft system

I. Introduction

SPACECRAFT simulations are critical to any mission, from CubeSats to deep space missions. They enable detailed analysis of the spacecraft's dynamics, ultimately informing how it will behave and if the mission requirements are met. As missions become more complex, so do the simulations for the spacecraft's behavior. For example, whereas many spacecraft use rigid solar panels, new missions such as the Lucy mission to the Trojan asteroids have started to use flexible solar panels [1] to meet higher power needs. Another example of this increased complexity relates to the main thruster platform. While many spacecraft attach the thruster directly to the system's hub, some have used a gimbaled platform instead. This is particularly useful for spacecraft using ionic thrusters [2], as they tend to thrust for long periods and need to account for offsets between the thrust vector and the center of mass. Missions like Deep Space 1 [3], Dawn [4], and Psyche [5] all use this technology. These mission-critical features add a layer of complexity that needs to be included in spacecraft simulations.

One of the critical steps in developing these comprehensive, high-fidelity simulations is deriving the spacecraft's translational and rotational equations of motion, which can be used in many different applications. Commercial structural dynamics solvers are very

Presented as Paper AAS 23-112 at the 2023 AAS Rocky Mountain GN&C Conference held in Breckenridge, CO, February 2–8, 2023; received 23 August 2023; revision received 8 January 2024; accepted for publication 14 January 2024; published online 29 March 2024.

*Graduate Research Assistant, Ann & H. J. Smead Department of Aerospace Engineering Sciences; joao.carneiro@colorado.edu. Member AIAA.
†Guidance, Navigation and Control Engineer, Laboratory for Atmospheric and Space Physics.
‡Schaden Leadership Chair, Professor, Ann & H. J. Smead Department of Aerospace Engineering Sciences. Fellow AIAA.

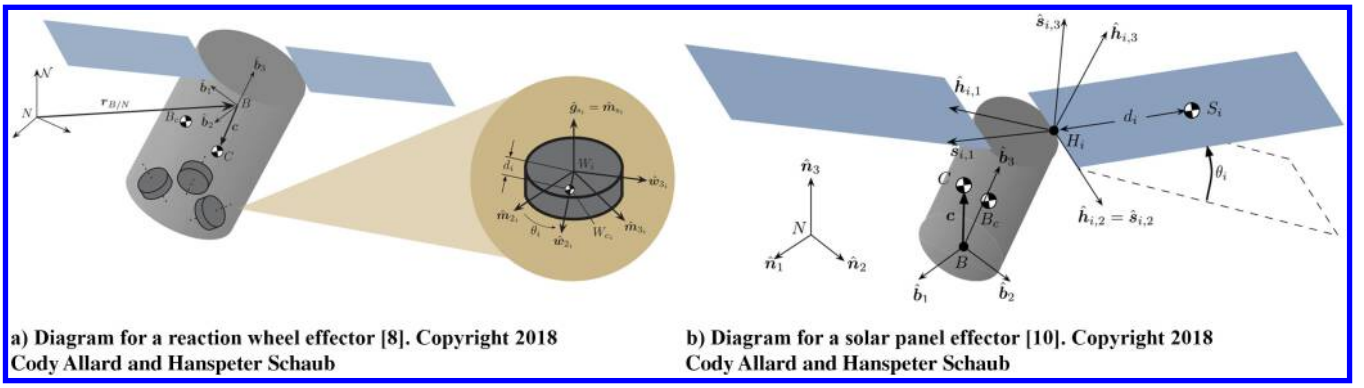

a) Diagram for a reaction wheel effector [8]. Copyright 2018 Cody Allard and Hanspeter Schaub

b) Diagram for a solar panel effector [10]. Copyright 2018 Cody Allard and Hanspeter Schaub

Fig. 1 Diagrams for two different single-axis components.

general in their spacecraft configuration space that they can model. Still, they are not readily configured to model spacecraft orbital and attitude motion subject to flight algorithms and sensor signals. This requires a more modular spacecraft simulation architecture. NASA's open-source 42 software[¶] can simulate spacecraft with multiple rigid-body subcomponents. However, the software requires creating the differential equations of motion for each new subsystem. The JPL closed-source Dshell software can also simulate spacecraft with multiple actuated components.[§] Here, an autocode generator step yields the equations of motion. By numerically propagating nonlinearly coupled differential equations of motion, the behavior of the spacecraft and its components can be analyzed, which can inform their performance during all mission phases. More recently, the spacecraft backsubstitution method (BSM) has been developed to rapidly create spacecraft simulations with multiple articulated rigid subcomponents [6]. This method avoids the challenging system mass matrix inverse by analytically backsolving for the dependencies of the rigid subcomponents onto a central spacecraft hub component. The result is a closed-form set of differential equations of motion that can be implemented modularly for rapid simulation prototyping and execution [7]. However, this approach is limited by the availability of analytical effector differential equations. The more general the effector solutions are, the more complex the spacecraft configuration can be with this BSM. The equations of motion can also be used to develop control laws to guarantee that the spacecraft stably performs within the desired metrics. Moreover, the equations of motion are a critical piece of state estimation and filtering, whether with respect to orbital maneuvers or attitude. These equations of motion must respect physical conservation laws, which are developed in Ref. [6]. Another critical aspect of simulation development is the software implementation of these equations, which is verified through energy and angular momentum conservation laws. A modular, general software architecture enables faster prototyping and guarantees the model's fidelity with increasing complexity.

Previous work with the spacecraft BSM has focused on the derivation of equations of motion in a modular way, separating each component's contributions by assuming they are connected directly to a common spacecraft's hub [6]. The time-varying rigid subcomponents are referred to as effectors. Some effector examples include reaction wheels [8], variable-speed control moment gyroscopes [9], and hinged solar arrays [10], which have symmetry constraints imposed. In prior work, the approach to derive the effector equations of motion relied on first making reasonable assumptions about the modeled component. To illustrate this, Fig. 1 shows diagrams of two rotating single-axis components: Fig. 1a shows the problem statement of a spacecraft with a reaction wheel, and Fig. 1b shows the problem statement of a spacecraft with a hinged panel.

To model the reaction wheel, some assumptions are placed on the wheel frame $\mathcal{W}$. The center of mass of the reaction wheel must lie in the $\boldsymbol{W}_2$–$\boldsymbol{W}_3$ plane. The wheel's frame is also defined so that the first axis aligns with the spin axis and the second axis with the center-of-mass offset. To model the solar panel, the frame's first axis is aligned with the center-of-mass offset, whereas the second axis is identical to the hinge axis.

The result is a set of equations of motion that represent each component individually. No further simplifications are done besides the ones resulting from the initial model assumptions. Although it is common to ignore some cross-coupling terms because their contribution is much smaller than the more dominant ones, the approaches presented in this paper and Refs. [6–11] retain the full equations. First, this enables closed-form equations of motion solutions for much more complex rotating subcomponents, which can readily be simulated without autocoding or deriving spacecraft equations of motion. The solutions are analytical. Second, this allows the verification of each model using energy and momentum conservation laws, as the solutions are fully coupled nonlinear solutions.

The main limitation of the work in Refs. [6–11] is that the equations of motion are specific to each component, even when different effectors represent the same rotating or spinning rigid body from a dynamic standpoint. Using the example of a reaction wheel and a solar panel, they both represent rigid bodies rotating about a single hinge. However, the initial assumptions on the center-of-mass offset, spin axis, etc., defined before developing the equations of motion yield distinct formulations. This means that the equations of motion have to be derived, implemented, and verified for each element. Moreover, while these equations can be implemented modularly, the software implementation also relies on specifying the type of component in the model. Further, they always assume that the rigid subcomponent is performing a single-degree-of-freedom (single-DoF) rotation relative to the parent component. This restricts the spacecraft configuration space that can be modeled.

This paper aims to derive and implement the general equations of motion for rotating body components with one or 2 degrees of freedom in the most general manner possible while still leveraging the benefits of the BSM, like its modularity and speed. Symmetry assumptions and center-of-mass constraints of prior work are removed. Rotating bodies with 1-DoF include reaction wheels and single-hinged solar panels. Similarly, control moment gyroscopes and dual-gimbaled thrusters are considered 2-DoF components. However, in contrast to prior 2-DoF effector solutions, these can have arbitrary mass distributions, such as mass and inertia, as well as the rotating axis. This abstraction means that the same general formulation can be used for any component that fits the specifications of a single- or dual-axis rotating rigid body. This dramatically expands the spacecraft dynamics design and configuration space; instead of having to model new components from scratch, the general model can be used.

The resulting formulation follows the BSM [6,7,10,11], which requires analytically substituting the effector equations of motion to decouple them from the hub equations of motion, thus avoiding inverting huge system mass matrices. Instead, each additional equation of motion beyond the spacecraft's translational and rotational equations is written in terms of the system's acceleration and angular velocity $\ddot{\boldsymbol{r}}_{B/N}$ and $\dot{\boldsymbol{\omega}}_{\mathcal{B}/\mathcal{N}}$, respectively. These terms are "backsubstituted" in such a way that $\ddot{\boldsymbol{r}}_{B/N}$ and $\dot{\boldsymbol{\omega}}_{\mathcal{B}/\mathcal{N}}$ can be solved for separately,

[¶]Data available online at https://software.nasa.gov/software/GSC-16720-1.
[§]Data available online at https://dartslab.jpl.nasa.gov/DSHELL.

and then solve all other degrees of freedom. The full detailed description of this method is given in Ref. [6].

To find the general equations of motion of the spacecraft system without making any assumptions about the rotating rigid bodies, the inertia tensor transport theorem is applied extensively [12]. This theorem converts the time derivative of the inertia tensor expressed in one frame to another frame, which is analogous to the vector transport theorem [13]. This theorem has no assumptions about the frame needed to derive the spacecraft's equations of motion. This is crucial for the general formulation of the equations describing rotating rigid-body classes.

The outcome of this work is a general analytical description of these rotating bodies that is agnostic to the type of rotating body being simulated. These results can be applied to various scenarios, and the proposed architecture can be implemented in any software package, such as DARTS, or even as a custom MATLAB/Simulink module. In particular, Basilisk,[**] the open-source, spacecraft-centric simulation software, is the chosen package used for software implementation in this work. It includes modular spacecraft dynamics and flight software modules and has been extensively used in mission analysis. The Laboratory of Atmospheric and Space Physics (LASP) is a codeveloper of the open-source Basilisk astrodynamics simulation framework and is using this tool in its mission development work. Moreover, private companies like U-Space [14] and AstroScale [15] have also used Basilisk for their own missions.

The general formulations presented in this work save development time, as only one set of equations needs to be derived. They allow for much faster prototyping of new components that conform to the specifications of single- or dual-axis parts, as the underlying equations are identical. Moreover, they also facilitate the verification process. For example, instead of verifying every different component (with the same number of degrees of freedom), the common functions, such as equations of motion, mass properties, and energy and momentum contributions, can be verified using the general formulation. For example, instead of verifying the implementation of the reaction wheel, solar panel, and one-axis antenna modules, the general 1-DoF module is verified, which can simulate all these different components. The same reasoning can be applied to the 2-DoF formulation. For a more detailed description of the software implementation of the formulation of the proposed dynamics, see Ref. [16].

This paper is organized as follows: First, the problem statement and equations of motion for the 1-DoF system are shown. Then, this process is repeated for the 2-DoF system. Finally, a numerical simulation shows how a single general formulation can be applied to different components. The Appendix section presents the verification of the equations of motion by demonstrating that energy and angular momentum are conserved for the example problem.

II. Backsubstitution Method

The backsubstitution method (BSM) is a dynamics formulation where the spacecraft equations of motion are written in a modular way. It is well-suited for single-spacecraft configurations consisting of a rigid hub with multiple appendages, also called effectors, attached to it. By separating the explicit and implicit second-order terms and grouping spacecraft mass quantities, the contributions of all effectors can be summed over each effector in parallel, enabling the simulation of any number of effectors and giving rise to the modularity of the equations of motion. This result is useful in spacecraft dynamics because spacecraft are often built using a rigid hub to which multiple components are attached, which fits the assumption in the BSM. The BSM speed and modularity benefits arise from taking advantage of this assumed underlying structure of having a rigid hub to which other effectors are attached. However, this method assumes the complex analytical backsubstitution process has been developed for an effector model.

Beyond this, the BSM also increases the speed of propagating the equations of motion. Instead of inverting a single mass matrix to solve for all second-order state variables, the system of equations can be solved by separating the hub's position and attitude from each effector's unique equation of motion. This is possible because of the unique structure of the system mass matrix under the assumption of one hub with multiple parallel effectors, which is shown in Eq. (1): each effector has a direct coupling with the hub's states and vice versa, but each effector does not couple with others. Therefore, the mass matrix's first six rows and columns are fully populated, while the remaining mass matrix is block diagonal. Instead of inverting an $N \times N$ matrix (for N total degrees of freedom), the backsubstitution only inverts a 6×6 matrix plus any smaller mass matrices for the effectors. Because matrix inversion is an N^3 process, separating this into smaller matrices is an enormous computational effort saver.

$$\begin{bmatrix} [\cdot]_{3\times3} & [\cdot]_{3\times3} & [\cdot]_{3\times N_1} & [\cdot]_{3\times N_2} & \cdots & [\cdot]_{3\times N_e} \\ [\cdot]_{3\times3} & [\cdot]_{3\times3} & [\cdot]_{3\times N_1} & [\cdot]_{3\times N_2} & \cdots & [\cdot]_{3\times N_e} \\ [\cdot]_{N_1\times3} & [\cdot]_{N_1\times3} & [\cdot]_{N_1\times N_1} & [0]_{N_1\times N_2} & \cdots & [0]_{N_1\times N_e} \\ [\cdot]_{N_2\times3} & [\cdot]_{N_2\times3} & [0]_{N_2\times N_1} & [\cdot]_{N_2\times N_2} & \cdots & [0]_{N_2\times N_e} \\ \vdots & \vdots & \vdots & \vdots & \ddots & \vdots \\ [\cdot]_{N_e\times3} & [\cdot]_{N_e\times3} & [0]_{N_e\times N_1} & [0]_{N_e\times N_2} & \cdots & [\cdot]_{N_e\times N_e} \end{bmatrix} \begin{bmatrix} \ddot{\boldsymbol{r}}_{B/N} \\ \dot{\boldsymbol{\omega}}_{\mathcal{B}/\mathcal{N}} \\ \boldsymbol{\alpha}_1 \\ \boldsymbol{\alpha}_2 \\ \vdots \\ \boldsymbol{\alpha}_e \end{bmatrix} = \begin{bmatrix} [\cdot]_{3\times1} \\ [\cdot]_{3\times1} \\ [\cdot]_{N_1\times1} \\ [\cdot]_{N_2\times1} \\ \vdots \\ [\cdot]_{N_e\times1} \end{bmatrix} \tag{1}$$

One of the drawbacks of the BSM relates to the assumption that all effectors are connected through the hub in parallel. It is impossible to chain effectors in series, like in parallel, because the effectors would cross-couple with each other, and the effector portion of the mass matrix would no longer be block diagonal. Therefore, to increase the degrees of freedom of a particular effector, it is necessary to rederive the equations of motion for the intended configuration. This is why there is a derivation of the equations of motion for one and 2-DoF effectors since it is impossible to stack two 1-DoF effectors to get the results for a dual-axis effector.

The equations of motion must be written in a specific way to apply the BSM [6]. The translational equation of motion is

$$m_{\text{sc}}\ddot{\boldsymbol{r}}_{B/N} - m_{\text{sc}}[\tilde{\boldsymbol{c}}]\dot{\boldsymbol{\omega}}_{\mathcal{B}/\mathcal{N}} + \sum_{i=1}^{N_{\text{eff}}}\sum_{j=1}^{N_{\text{DOF},i}} \boldsymbol{v}_{\text{Trans,LHS}_{ij}}\ddot{\alpha}_{ij} = \boldsymbol{F}_{\text{ext}} - 2m_{\text{sc}}[\tilde{\boldsymbol{\omega}}_{\mathcal{B}/\mathcal{N}}]\boldsymbol{c}' - m_{\text{sc}}[\tilde{\boldsymbol{\omega}}_{\mathcal{B}/\mathcal{N}}][\tilde{\boldsymbol{\omega}}_{\mathcal{B}/\mathcal{N}}]\boldsymbol{c} + \sum_{i=1}^{N_{\text{eff}}}\boldsymbol{v}_{\text{Trans,RHS}_i} \tag{2}$$

The rotational equation of motion is

$$m_{\text{sc}}[\tilde{\boldsymbol{c}}]\ddot{\boldsymbol{r}}_{B/N} + [I_{\text{sc},B}]\dot{\boldsymbol{\omega}}_{\mathcal{B}/\mathcal{N}} + \sum_{i=1}^{N_{\text{eff}}}\sum_{j=1}^{N_{\text{DOF},i}} \boldsymbol{v}_{\text{Rot,LHS}_{ij}}\ddot{\alpha}_{ij} = \boldsymbol{L}_B - [\tilde{\boldsymbol{\omega}}_{\mathcal{B}/\mathcal{N}}][I_{\text{sc},B}]\boldsymbol{\omega}_{\mathcal{B}/\mathcal{N}} - [I'_{\text{sc},B}]\boldsymbol{\omega}_{\mathcal{B}/\mathcal{N}} + \sum_{i=1}^{N_{\text{eff}}}\boldsymbol{v}_{\text{Rot,RHS}_i} \tag{3}$$

The effector equation of motion is written as

$$\ddot{\alpha}_{ij} = \boldsymbol{a}_{ij}\cdot\ddot{\boldsymbol{r}}_{B/N} + \boldsymbol{b}_{ij}\cdot\dot{\boldsymbol{\omega}}_{\mathcal{B}/\mathcal{N}} + c_{ij} \tag{4}$$

where α_{ij} corresponds to the jth DoF of the ith effector. The $\boldsymbol{a}_{ij}$, $\boldsymbol{b}_{ij}$, and $\boldsymbol{c}_{ij}$ terms correspond to mass and inertia contributions. In the equations above, the dot and apostrophe denote the inertial and body-frame derivatives, respectively. Note that while some terms are explicit effector contributions, namely those that are part of summations, others include implicit effector contributions. These consist of the mass properties of the overall spacecraft: $\boldsymbol{c}$ and $\boldsymbol{c}'$, the position vector between the center of mass of the system and point B and its body-frame derivative, as well as $[I_{\text{sc},B}]$ and $[I'_{\text{sc},B}]$, the inertia of the spacecraft about point B and its body-frame derivative. Therefore, each effector must compute its contributions to the spacecraft's mass properties at each timestep to compute the updated mass and inertia quantities.

**Data available online at http://hanspeterschaub.info/basilisk.

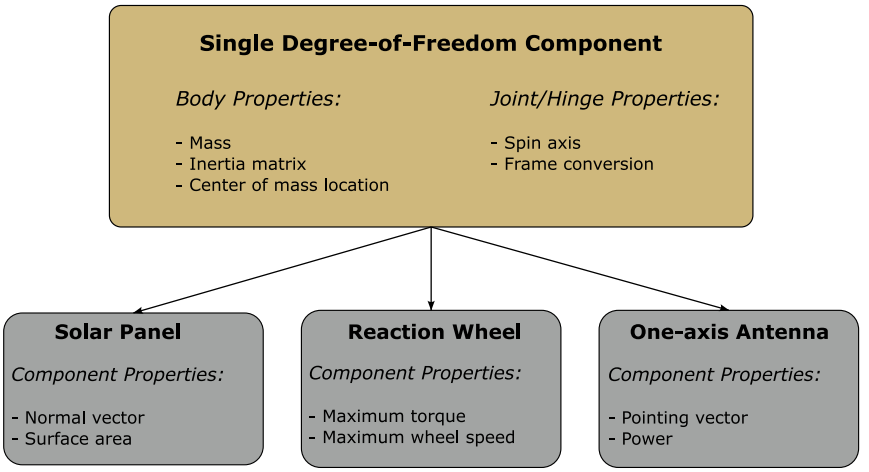

Fig. 2 Diagram for the one-axis rotating rigid-body class.

As shown, the goal of writing the equations in the presented form is to apply the BSM. Taking Eq. (4), the $\ddot{\alpha}$ term can be "back-substituted" directly into Eqs. (2) and (3). This results in two sets of equations that only depend on $\ddot{\boldsymbol{r}}_{B/N}$ and $\dot{\boldsymbol{\omega}}_{\mathcal{B}/\mathcal{N}}$, which can be used to solve for those two quantities directly. Finally, once $\ddot{\boldsymbol{r}}_{B/N}$ and $\dot{\boldsymbol{\omega}}_{\mathcal{B}/\mathcal{N}}$ are known, they can be substituted back into Eq. (4), which yields a solution $\ddot{\alpha}$. All second-order state variables are known, which can be numerically propagated using a fourth-order Runge–Kutta numerical integrator.

III. Single-Axis Rotating Rigid-Body Dynamics

This section describes the derivation of the equations of motion of a single-axis rotating rigid body attached to a rigid hub. It introduces the generality of the problem statement by making fewer assumptions on the simulated component than previous work on backsubstitution while leveraging results such as the inertia transport theorem to find the resulting equations of motion. The 1-DoF component is a rigid body that can only rotate about one body-fixed axis through a rotary joint. This general description can describe multiple common spacecraft components. Examples include single-hinge solar arrays for deployment or first-order flexing analysis, reaction wheels as attitude control devices, and one-axis gimbaled low-gain antennas. These components can be defined through a general description, specified by their mass, inertia matrix, location of the center of mass, and spin axis. The module's Basilisk framework implementation can be found here.[††] Note that, while the backsubstitution effector solution is modeled in this paper using the Basilisk software [17], the underlying math is agnostic to this software implementation.

A diagram for the single-axis rotating rigid body is shown in Fig. 2 as a gold box. It represents the skeleton for rigid spacecraft appendages that rotate about one axis. Several properties, such as the body's mass and inertia matrix, are common to all single-axis rotating rigid bodies. The center-of-mass location and spin axis can be defined as any vectors without any assumptions on how the frame is determined. The frame conversion information relating the rotating rigid-body frame to the body-fixed frame is expressed through a direction cosine matrix (DCM). This generality enables using common equations of motion that describe the system, mass property contributions to compute the spacecraft's center of mass and inertia matrix, and energy and momentum contributions to calculate the spacecraft's total energy and angular momentum.

The gray boxes represent specific modules that can be derived from the general 1-DoF formulation. These include hinged solar panels, reaction wheels, or one-axis gimbaled antennas. These modules use the 1-DoF formulation, which means they all contain the same properties from the parent structure. Adding new component properties that define that particular component type can specify each unique element. For example, a solar panel needs a vector normal to the solar cells to point at the sun, as well as the total surface area of the solar cells. Adding additional parameters makes the module more specific while retaining the structure common to all single-axis rotating rigid bodies.

Although the proposed method is agnostic to any dynamics formulation, this work uses a Newtonian/Eulerian approach to derive the motion equations. This means that the translational equations of motion use the super particle theorem, or Newton's second law, while the rotational equations use Euler's rotation equations [13]. The derivations begin by considering the entire system to develop its translational and rotational equations of motion. The components are then considered separately, where their rotational motion equation is developed. Different approaches to arrive at the same results exist. For example, in Lagrange mechanics [18], the potential and kinetic energy are used in the Lagrangian function, applying the Lagrange equations of the first kind. Kane's method [19,20] uses the concept of generalized forces and generalized inertia forces to create a systematic formulation suited for multibody systems and is easy to implement in software. Spatial operator logic [21] is another method that has been applied to deriving the equations of motion spacecraft, with particular importance to multibody robotic systems [22] and flexible components [23]. The Jet Propulsion Laboratory has developed DARTS,[‡‡] which uses spatial operator algebra for its simulations.

A. Problem Statement

The problem statement for the single-axis rotating rigid body is illustrated in Fig. 3. The inertial frame is represented by $\mathcal{N}$ with origin at point N. The spacecraft is composed of a rigid body connected to a rigid hub through a single axis of rotation. The hub has a body-fixed frame $\mathcal{B}$ with origin B, and its center of mass is at point B_c. The mass of the hub is m_{hub}, and its inertia tensor about point B is $[I_{\text{hub},B}]$. The rotating rigid body has the $\mathcal{S}$ frame attached to it with its origin at point S. The center of mass of the spinner is located at point S_c. The mass of the spinner is m_{S}, and its inertia tensor about its center of mass is $[I_{\text{S},S_c}]$. The combined center of mass of the system is located at point C. The spin axis $\hat{\boldsymbol{s}}$ is constant, as seen by the $\mathcal{B}$ frame, and passes through point S. This means that the position of point S does not change as seen from the hub since the axis of rotation passes through it. The angle about the rotation axis is θ, and its angle rate is $\dot{\theta}$.

The single-axis rotating rigid body attached to the hub has 7 degrees of freedom, as shown in Table 1: three for the system's position, three for the system's attitude, and one for the angle about the rotation axis. The motion equations are developed so that all

[††]Data available online at https://hanspeterschaub.info/basilisk/Documentation/simulation/dynamics/spinningBodies/spinningBodiesOneDOF/spinningBodyOneDOFStateEffector.html.

[‡‡]Data available online at https://dartslab.jpl.nasa.gov/DSHELL/index.php.

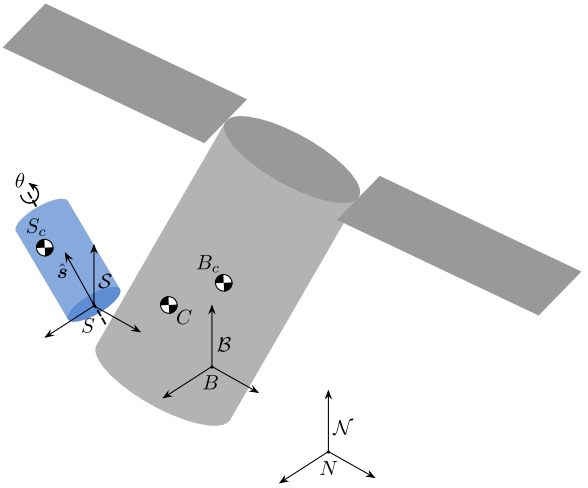

Fig. 3 Problem statement for the 1-DoF spinning rigid body.

Table 1 State variables for the single-axis rotating rigid-body spacecraft

State variables	Degrees of freedom	Equations of motion
$\boldsymbol{r}_{B/N}, \dot{\boldsymbol{r}}_{B/N}$	3	Translational
$\boldsymbol{\sigma}_{\mathcal{B}/\mathcal{N}}, \boldsymbol{\omega}_{\mathcal{B}/\mathcal{N}}$	3	Rotational
$\theta, \dot{\theta}$	1	Spinner rotational

degrees of freedom are described. The position state variables are defined by the translational equation of motion, the attitude state variables by the rotational equation of motion, and the rotation angle by the spinner equation of motion.

B. Translational Equations of Motion

The entire system is considered for the translational equation of motion, including the hub and the spinner. This equation of motion defines 3 degrees of freedom of the system. Using the super particle theorem

$$m_{\text{sc}}\ddot{\boldsymbol{r}}_{C/N} = m_{\text{sc}}\ddot{\boldsymbol{r}}_{B/N} + m_{\text{sc}}\ddot{\boldsymbol{c}} = \boldsymbol{F}_{\text{ext}} \tag{5}$$

where $\boldsymbol{c} \equiv \boldsymbol{r}_{C/B}$ is the vector from the origin of the body frame B to the system's center of mass C, and $\boldsymbol{F}_{\text{ext}}$ is the combined force acting on the system. A single dot above a vector represents the first-order inertial frame derivative, and a double dot represents the second-order inertial frame derivative. Using the definition of the center of mass of the system

$$m_{\text{sc}}\boldsymbol{c} = m_{\text{hub}}\boldsymbol{r}_{B_c/B} + m_{\text{S}}\boldsymbol{r}_{S_c/B} \tag{6}$$

and using the transport theorem, the inertial time derivatives are expressed using body-frame derivatives as

$$\dot{\boldsymbol{c}} = \boldsymbol{c}' + \boldsymbol{\omega}_{\mathcal{B}/\mathcal{N}} \times \boldsymbol{c} \tag{7}$$

$$\ddot{\boldsymbol{c}} = \boldsymbol{c}'' + \dot{\boldsymbol{\omega}}_{\mathcal{B}/\mathcal{N}} \times \boldsymbol{c} + \boldsymbol{\omega}_{\mathcal{B}/\mathcal{N}} \times \boldsymbol{c}' + \boldsymbol{\omega}_{\mathcal{B}/\mathcal{N}} \times \dot{\boldsymbol{c}} \tag{8}$$

where a single apostrophe represents a first-order body-frame derivative and a double apostrophe represents a second-order body-frame derivative. The term $\boldsymbol{\omega}_{\mathcal{B}/\mathcal{N}}$ represents the angular velocity of the $\mathcal{B}$ frame relative to the $\mathcal{N}$ frame. As for the body-frame time derivatives, the $\boldsymbol{r}_{B_c/B}$ and $\boldsymbol{r}_{S/B}$ vectors are fixed with respect to the $\mathcal{B}$ frame ($\boldsymbol{r}'_{B_c/B} = \boldsymbol{r}'_{S/B} = \boldsymbol{0}$) because the $\mathcal{B}$ frame is attached to the rigid hub and $\hat{\boldsymbol{s}}$ passes through point S. It follows that

$$m_{\text{sc}}\boldsymbol{c}' = m_{\text{S}}\boldsymbol{r}'_{S_c/B} = m_{\text{S}}\boldsymbol{r}'_{S_c/S} = m_{\text{S}}\boldsymbol{\omega}_{\mathcal{S}/\mathcal{B}} \times \boldsymbol{r}_{S_c/S} \tag{9}$$

$$m_{\text{sc}}\boldsymbol{c}'' = m_{\text{S}}\left(\ddot{\theta}\,\hat{\boldsymbol{s}} \times \boldsymbol{r}_{S_c/S} + \boldsymbol{\omega}_{\mathcal{S}/\mathcal{B}} \times \boldsymbol{r}'_{S_c/S}\right) \tag{10}$$

where by definition

$$\boldsymbol{\omega}_{\mathcal{S}/\mathcal{B}} = \dot{\theta}\,\hat{\boldsymbol{s}}, \quad \boldsymbol{\omega}'_{\mathcal{S}/\mathcal{B}} = \ddot{\theta}\,\hat{\boldsymbol{s}} \tag{11}$$

because $\hat{\boldsymbol{s}}$ is fixed in the $\mathcal{B}$ frame. Finally, all these terms are combined to yield

$$\begin{aligned} m_{\text{sc}}\ddot{\boldsymbol{r}}_{\mathcal{B}/\mathcal{N}} - m_{\text{sc}}[\tilde{\boldsymbol{c}}]\dot{\boldsymbol{\omega}}_{\mathcal{B}/\mathcal{N}} - m_{\text{S}}[\tilde{\boldsymbol{r}}_{S_c/S}]\hat{\boldsymbol{s}}\,\ddot{\theta} &= \boldsymbol{F}_{\text{ext}} - 2m_{\text{sc}}[\tilde{\boldsymbol{\omega}}_{\mathcal{B}/\mathcal{N}}]\boldsymbol{c}' \\ &\quad - m_{\text{sc}}[\tilde{\boldsymbol{\omega}}_{\mathcal{B}/\mathcal{N}}][\tilde{\boldsymbol{\omega}}_{\mathcal{B}/\mathcal{N}}]\boldsymbol{c} - m_{\text{S}}[\tilde{\boldsymbol{\omega}}_{\mathcal{S}/\mathcal{B}}]\boldsymbol{r}'_{S_c/S} \end{aligned} \tag{12}$$

In the equation above, the matrix cross-product operator is used. For an arbitrary vector $\boldsymbol{a} = [a_1, a_2, a_3]^T$, the corresponding matrix cross product operator is written as $[\tilde{\boldsymbol{a}}]$ and is given by

$$[\tilde{\boldsymbol{a}}] = \begin{bmatrix} 0 & -a_3 & a_2 \\ a_3 & 0 & -a_1 \\ -a_2 & a_1 & 0 \end{bmatrix} \tag{13}$$

C. Rotational Equations of Motion

For the rotational equation of motion, the entire spacecraft is considered. This equation of motion defines 3 degrees of freedom of the system. The rotational differential equation given about point B, which is not the system's center of mass, is given by

$$\dot{\boldsymbol{H}}_{\text{sc},B} = \boldsymbol{L}_B + m_{\text{sc}}\ddot{\boldsymbol{r}}_{B/N} \times \boldsymbol{c} \tag{14}$$

where $\boldsymbol{H}_{\text{sc},B}$ is the angular momentum of the spacecraft (sc) about point B and $\boldsymbol{L}_B$ is the torque about point B. The angular momentum is

$$\begin{aligned} \boldsymbol{H}_{\text{sc},B} &= \boldsymbol{H}_{\text{hub},B} + \boldsymbol{H}_{S,B} \\ &= [I_{\text{hub},B}]\boldsymbol{\omega}_{\mathcal{B}/\mathcal{N}} + [I_{\text{S},S_c}]\boldsymbol{\omega}_{\mathcal{S}/\mathcal{N}} + m_{\text{S}}\boldsymbol{r}_{S_c/B} \times \dot{\boldsymbol{r}}_{S_c/B} \end{aligned} \tag{15}$$

where $\boldsymbol{H}_{\text{hub},B}$ is the angular momentum of the hub and $\boldsymbol{H}_{S,B}$ is the angular momentum of the spinner, both about point B. The terms multiplied by $\boldsymbol{\omega}_{\mathcal{B}/\mathcal{N}}$ are grouped to simplify the expression above. To express the inertial time derivative using the $\mathcal{B}$ frame time derivative, the equality $\boldsymbol{\omega}_{\mathcal{S}/\mathcal{N}} = \boldsymbol{\omega}_{\mathcal{S}/\mathcal{B}} + \boldsymbol{\omega}_{\mathcal{B}/\mathcal{N}}$ and $\dot{\boldsymbol{r}}_{S_c/B} = \boldsymbol{r}'_{S_c/B} + \boldsymbol{\omega}_{\mathcal{B}/\mathcal{N}} \times \boldsymbol{r}_{S_c/B}$ is used, which yields

$$\boldsymbol{H}_{\text{sc},B} = [I_{\text{sc},B}]\boldsymbol{\omega}_{\mathcal{B}/\mathcal{N}} + [I_{\text{S},S_c}]\boldsymbol{\omega}_{\mathcal{S}/\mathcal{B}} + m_{\text{S}}\boldsymbol{r}_{S_c/B} \times \boldsymbol{r}'_{S_c/B} \tag{16}$$

where the spacecraft's total inertia about point B can be found using the parallel axis theorem and is given by

$$[I_{\text{sc},B}] = [I_{\text{hub},B}] + [I_{\text{S},S_c}] - m_{\text{S}}[\tilde{\boldsymbol{r}}_{S_c/B}][\tilde{\boldsymbol{r}}_{S_c/B}] \tag{17}$$

The inertial time derivative of the total angular momentum is expressed as

$$\begin{aligned} \dot{\boldsymbol{H}}_{\text{sc},B} &= [I_{\text{sc},B}]\dot{\boldsymbol{\omega}}_{\mathcal{B}/\mathcal{N}} + [I'_{\text{sc},B}]\boldsymbol{\omega}_{\mathcal{B}/\mathcal{N}} + \boldsymbol{\omega}_{\mathcal{B}/\mathcal{N}} \times [I_{\text{sc},B}]\boldsymbol{\omega}_{\mathcal{B}/\mathcal{N}} \\ &\quad + [I_{\text{S},S_c}]\ddot{\theta}\,\hat{\boldsymbol{s}} + \boldsymbol{\omega}_{\mathcal{S}/\mathcal{N}} \times [I_{\text{S},S_c}]\boldsymbol{\omega}_{\mathcal{S}/\mathcal{B}} + m_{\text{S}}\boldsymbol{r}_{S_c/B} \times \boldsymbol{r}''_{S_c/B} \\ &\quad + m_{\text{S}}\boldsymbol{\omega}_{\mathcal{B}/\mathcal{N}} \times (\boldsymbol{r}_{S_c/B} \times \boldsymbol{r}'_{S_c/B}) \end{aligned} \tag{18}$$

Some terms are defined before writing the final equation to yield a notationally compact solution description. The inertia transport theorem needs to be used to take the body-frame time derivative of the total spacecraft inertia. The time derivative of the inertia tensor $[I]$ with respect to the $\mathcal{A}$ frame can be written using the time derivative with respect to the $\mathcal{B}$ frame as [12]

$$\frac{{}^{\mathcal{A}}d}{dt}[I] = \frac{{}^{\mathcal{B}}d}{dt}[I] + [\tilde{\boldsymbol{\omega}}_{\mathcal{B}/\mathcal{A}}][I] - [I][\tilde{\boldsymbol{\omega}}_{\mathcal{B}/\mathcal{A}}] \tag{19}$$

With this result, the body-frame time derivative of the total spacecraft inertia is

$$\begin{aligned}[I'_{\mathrm{sc},B}] &= [I'_{\mathrm{sc},S_c}] - m_{\mathrm{S}}[\tilde{\boldsymbol{r}}'_{S_c/B}][\tilde{\boldsymbol{r}}_{S_c/B}] - m_{\mathrm{S}}[\tilde{\boldsymbol{r}}_{S_c/B}][\tilde{\boldsymbol{r}}'_{S_c/B}] \\ &= [\tilde{\boldsymbol{\omega}}_{\mathcal{S}/\mathcal{B}}][I_{\mathrm{S},S_c}] - [I_{\mathrm{S},S_c}][\tilde{\boldsymbol{\omega}}_{\mathcal{S}/\mathcal{B}}] - m_{\mathrm{S}}[\tilde{\boldsymbol{r}}'_{S_c/B}][\tilde{\boldsymbol{r}}_{S_c/B}] \\ &\quad - m_{\mathrm{S}}[\tilde{\boldsymbol{r}}_{S_c/B}][\tilde{\boldsymbol{r}}'_{S_c/B}] \end{aligned} \tag{20}$$

The final equation includes four distinct terms. The first two relate to the time rate of change of the inertia about the center of mass (point S_c), which is calculated using Eq. (19). Note that the first term in the theorem is not present because the inertia is constant, as seen from the $\mathcal{S}$ frame. The second two terms result from the parallel axis theorem. From Eq. (17), taking the $\mathcal{B}$ frame derivative of the last term results in these two additional terms using the derivative chain rule.

Because $\boldsymbol{r}''_{S_c/B}$ contains second-order terms, it must be simplified to

$$\boldsymbol{r}''_{S_c/B} = \boldsymbol{r}''_{S_c/S} = \ddot{\theta}\hat{\boldsymbol{s}} \times \boldsymbol{r}_{S_c/S} + \boldsymbol{\omega}_{\mathcal{S}/\mathcal{B}} \times \boldsymbol{r}'_{S_c/S} \tag{21}$$

Combining these results into the rotational equation of motion yields the final expression for the rotational equation of motion:

$$\begin{aligned} &m_{\mathrm{sc}}[\tilde{\boldsymbol{c}}]\ddot{\boldsymbol{r}}_{\mathcal{B}/\mathcal{N}} + [I_{\mathrm{sc},B}]\dot{\boldsymbol{\omega}}_{\mathcal{B}/\mathcal{N}} + \left([I_{\mathrm{S},S_c}] - m_{\mathrm{S}}[\tilde{\boldsymbol{r}}_{S_c/B}][\tilde{\boldsymbol{r}}_{S_c/S}]\right)\hat{\boldsymbol{s}}\,\ddot{\theta} \\ &= \boldsymbol{L}_B - [\tilde{\boldsymbol{\omega}}_{\mathcal{B}/\mathcal{N}}][I_{\mathrm{sc},B}]\boldsymbol{\omega}_{\mathcal{B}/\mathcal{N}} - [I'_{\mathrm{sc},B}]\boldsymbol{\omega}_{\mathcal{B}/\mathcal{N}} - [\tilde{\boldsymbol{\omega}}_{\mathcal{S}/\mathcal{N}}][I_{\mathrm{S},S_c}]\boldsymbol{\omega}_{\mathcal{S}/\mathcal{B}} \\ &\quad - m_{\mathrm{S}}[\tilde{\boldsymbol{\omega}}_{\mathcal{B}/\mathcal{N}}][\tilde{\boldsymbol{r}}_{S_c/B}]\boldsymbol{r}'_{S_c/B} - m_{\mathrm{S}}[\tilde{\boldsymbol{r}}_{S_c/B}][\tilde{\boldsymbol{\omega}}_{\mathcal{S}/\mathcal{B}}]\boldsymbol{r}'_{S_c/S} \end{aligned} \tag{22}$$

D. Spinning Body Equations of Motion

Only the rotating rigid body is considered for the final equation of motion. This solves the final DoF of the system. The general formulation of the equation of motion of the spinning body is

$$\dot{\boldsymbol{H}}_{\mathrm{S},S} = \boldsymbol{L}_S - m_{\mathrm{S}}\boldsymbol{r}_{S_c/S} \times \ddot{\boldsymbol{r}}_{S/N} \tag{23}$$

The angular momentum of the spinner about point S is

$$\boldsymbol{H}_{\mathrm{S},S} = [I_{\mathrm{S},S}]\boldsymbol{\omega}_{\mathcal{S}/\mathcal{N}} \tag{24}$$

where $[I_{\mathrm{S},S}]$ is defined using the parallel axis theorem as $[I_{\mathrm{S},S}] = [I_{\mathrm{S},S_c}] - m_{\mathrm{S}}[\tilde{\boldsymbol{r}}_{S_c/S}][\tilde{\boldsymbol{r}}_{S_c/S}]$. The inertial time derivative of the angular momentum is given by

$$\dot{\boldsymbol{H}}_{\mathrm{S},S} = [I_{\mathrm{S},S}]\dot{\boldsymbol{\omega}}_{\mathcal{S}/\mathcal{N}} + \boldsymbol{\omega}_{\mathcal{S}/\mathcal{N}} \times [I_{\mathrm{S},S}]\boldsymbol{\omega}_{\mathcal{S}/\mathcal{N}} \tag{25}$$

As for the $\ddot{\boldsymbol{r}}_{S/N}$ term, it can be separated into two terms:

$$\ddot{\boldsymbol{r}}_{S/N} = \ddot{\boldsymbol{r}}_{S/B} + \ddot{\boldsymbol{r}}_{B/N} \tag{26}$$

To compute $\ddot{\boldsymbol{r}}_{S/B}$, the fact that $\boldsymbol{r}_{S/B}$ is constant in the $\mathcal{B}$ frame is used to yield

$$\dot{\boldsymbol{r}}_{S/B} = \boldsymbol{\omega}_{\mathcal{B}/\mathcal{N}} \times \boldsymbol{r}_{S/B} \tag{27}$$

$$\ddot{\boldsymbol{r}}_{S/B} = \dot{\boldsymbol{\omega}}_{\mathcal{B}/\mathcal{N}} \times \boldsymbol{r}_{S/B} + \boldsymbol{\omega}_{\mathcal{B}/\mathcal{N}} \times \dot{\boldsymbol{r}}_{S/B} \tag{28}$$

The term $\dot{\boldsymbol{\omega}}_{\mathcal{S}/\mathcal{N}}$ can be separated into three distinct terms:

$$\dot{\boldsymbol{\omega}}_{\mathcal{S}/\mathcal{N}} = \dot{\boldsymbol{\omega}}_{\mathcal{B}/\mathcal{N}} + \ddot{\theta}\hat{\boldsymbol{s}} + \boldsymbol{\omega}_{\mathcal{B}/\mathcal{N}} \times \boldsymbol{\omega}_{\mathcal{S}/\mathcal{B}} \tag{29}$$

Before these results are combined, the dot product with the spin axis $\hat{\boldsymbol{s}}$ is applied to all terms. This isolates the independent equation of motion along the axis of interest corresponding to the remaining DoF. When the dot product is applied, the original $\boldsymbol{L}_S$ term, which encompasses all torques applied to the spinning body, becomes u_S, which corresponds to the torque about the torque about the spin axis. This torque includes control torques and rotational springs and dampers along the spinning axis. The torques in other directions are structural and keep the single-axis rotation constraint in place. This approach consists of a minimal coordinate set formulation since the structural torques do not allow motion in other directions. This results in the following equation of motion:

$$\begin{aligned} \hat{\boldsymbol{s}}^T[I_{\mathrm{S},S}]\hat{\boldsymbol{s}}\,\ddot{\theta} &= u_S - m_{\mathrm{S}}\hat{\boldsymbol{s}}^T[\tilde{\boldsymbol{r}}_{S_c/S}]\ddot{\boldsymbol{r}}_{B/N} - \hat{\boldsymbol{s}}^T\left([I_{\mathrm{S},S}] - m_{\mathrm{S}}[\tilde{\boldsymbol{r}}_{S_c/S}][\tilde{\boldsymbol{r}}_{S/B}]\right)\dot{\boldsymbol{\omega}}_{\mathcal{B}/\mathcal{N}} \\ &\quad - \hat{\boldsymbol{s}}^T[\tilde{\boldsymbol{\omega}}_{\mathcal{S}/\mathcal{N}}][I_{\mathrm{S},S}]\boldsymbol{\omega}_{\mathcal{S}/\mathcal{N}} - \hat{\boldsymbol{s}}^T[I_{\mathrm{S},S}][\tilde{\boldsymbol{\omega}}_{\mathcal{B}/\mathcal{N}}]\boldsymbol{\omega}_{\mathcal{S}/\mathcal{B}} \\ &\quad - m_{\mathrm{S}}\hat{\boldsymbol{s}}^T[\tilde{\boldsymbol{r}}_{S_c/S}][\tilde{\boldsymbol{\omega}}_{\mathcal{B}/\mathcal{N}}]\dot{\boldsymbol{r}}_{S/B} \end{aligned} \tag{30}$$

E. Backsubstitution Formulation

The backsubstitution formulation must be defined to conform to the structure of the equations of motion in the BSM [6]. The spinning body equation of motion can be written in the form

$$\boldsymbol{m}_\theta\ddot{\theta} = \boldsymbol{a}^*_\theta \cdot \ddot{\boldsymbol{r}}_{B/N} + \boldsymbol{b}^*_\theta \cdot \dot{\boldsymbol{\omega}}_{\mathcal{B}/\mathcal{N}} + c^*_\theta \tag{31}$$

where the following terms are introduced

$$\boldsymbol{a}^*_\theta = m_{\mathrm{S}}[\tilde{\boldsymbol{r}}_{S_c/S}]\hat{\boldsymbol{s}} \tag{32}$$

$$\boldsymbol{b}^*_\theta = -([I_{\mathrm{S},S}] - m_{\mathrm{S}}[\tilde{\boldsymbol{r}}_{S/B}][\tilde{\boldsymbol{r}}_{S_c/S}])\hat{\boldsymbol{s}} \tag{33}$$

$$\begin{aligned} c^*_\theta = u_S &- \hat{\boldsymbol{s}}^T\left([\tilde{\boldsymbol{\omega}}_{\mathcal{S}/\mathcal{N}}][I_{\mathrm{S},S}]\boldsymbol{\omega}_{\mathcal{S}/\mathcal{N}} + [I_{\mathrm{S},S}][\tilde{\boldsymbol{\omega}}_{\mathcal{B}/\mathcal{N}}]\boldsymbol{\omega}_{\mathcal{S}/\mathcal{B}}\right. \\ &\left. + m_{\mathrm{S}}[\tilde{\boldsymbol{r}}_{S_c/S}][\tilde{\boldsymbol{\omega}}_{\mathcal{B}/\mathcal{N}}]\dot{\boldsymbol{r}}_{S/B}\right) \end{aligned} \tag{34}$$

along with the mass-like term $\boldsymbol{m}_\theta = \hat{\boldsymbol{s}}^T[I_{\mathrm{S},S}]\hat{\boldsymbol{s}}$. Using these terms, the spinning body equation of motion can be written in its compact form as

$$\ddot{\theta} = \boldsymbol{a}_\theta \cdot \ddot{\boldsymbol{r}}_{B/N} + \boldsymbol{b}_\theta \cdot \dot{\boldsymbol{\omega}}_{\mathcal{B}/\mathcal{N}} + c_\theta \tag{35}$$

where the new variables are defined as

$$\boldsymbol{a}_\theta = \frac{\boldsymbol{a}^*_\theta}{\boldsymbol{m}_\theta}, \quad \boldsymbol{b}_\theta = \frac{\boldsymbol{b}^*_\theta}{\boldsymbol{m}_\theta}, \quad \boldsymbol{c}_\theta = \frac{\boldsymbol{c}^*_\theta}{\boldsymbol{m}_\theta} \tag{36}$$

This result can be backsubstituted into Eqs. (12) and (22), which yields

$$\begin{bmatrix} [A] & [B] \\ [C] & [D] \end{bmatrix} \begin{bmatrix} \ddot{\boldsymbol{r}}_{B/N} \\ \dot{\boldsymbol{\omega}}_{\mathcal{B}/\mathcal{N}} \end{bmatrix} = \begin{bmatrix} \boldsymbol{v}_{\mathrm{trans}} \\ \boldsymbol{v}_{\mathrm{rot}} \end{bmatrix} \tag{37}$$

using the following matrices

$$[A] = m_{\mathrm{sc}}[I_{3\times3}] - m_{\mathrm{S}}[\tilde{\boldsymbol{r}}_{S_c/S}]\hat{\boldsymbol{s}}\boldsymbol{a}^T_\theta \tag{38}$$

$$[B] = -m_{\mathrm{sc}}[\tilde{\boldsymbol{c}}] - m_{\mathrm{S}}[\tilde{\boldsymbol{r}}_{S_c/S}]\hat{\boldsymbol{s}}\boldsymbol{b}^T_\theta \tag{39}$$

$$[C] = m_{\mathrm{sc}}[\tilde{\boldsymbol{c}}] + \left([I_{\mathrm{S},S_c}] - m_{\mathrm{S}}[\tilde{\boldsymbol{r}}_{S_c/B}][\tilde{\boldsymbol{r}}_{S_c/S}]\right)\hat{\boldsymbol{s}}a^T_\theta \tag{40}$$

$$[D] = [I_{\mathrm{sc},B}] + \left([I_{\mathrm{S},S_c}] - m_{\mathrm{S}}[\tilde{\boldsymbol{r}}_{S_c/B}][\tilde{\boldsymbol{r}}_{S_c/S}]\right)\hat{\boldsymbol{s}}b^T_\theta \tag{41}$$

and vectors

$$\begin{aligned} \boldsymbol{v}_{\mathrm{trans}} &= \boldsymbol{F}_{\mathrm{ext}} - 2m_{\mathrm{sc}}[\tilde{\boldsymbol{\omega}}_{\mathcal{B}/\mathcal{N}}]\boldsymbol{c}' - m_{\mathrm{sc}}[\tilde{\boldsymbol{\omega}}_{\mathcal{B}/\mathcal{N}}][\tilde{\boldsymbol{\omega}}_{\mathcal{B}/\mathcal{N}}]\boldsymbol{c} \\ &\quad - m_{\mathrm{S}}[\tilde{\boldsymbol{\omega}}_{\mathcal{S}/\mathcal{B}}]\boldsymbol{r}'_{S_c/S} + m_{\mathrm{S}}\boldsymbol{c}_\theta[\tilde{\boldsymbol{r}}_{S_c/S}]\hat{\boldsymbol{s}} \end{aligned} \tag{42}$$

$$\begin{aligned} \boldsymbol{v}_{\mathrm{rot}} &= \boldsymbol{L}_B - [\tilde{\boldsymbol{\omega}}_{\mathcal{B}/\mathcal{N}}][I_{\mathrm{sc},B}]\boldsymbol{\omega}_{\mathcal{B}/\mathcal{N}} - [I'_{\mathrm{sc},B}]\boldsymbol{\omega}_{\mathcal{B}/\mathcal{N}} - [\tilde{\boldsymbol{\omega}}_{\mathcal{S}/\mathcal{N}}][I_{\mathrm{S},S_c}]\boldsymbol{\omega}_{\mathcal{S}/\mathcal{B}} \\ &\quad - m_{\mathrm{S}}[\tilde{\boldsymbol{\omega}}_{\mathcal{B}/\mathcal{N}}][\tilde{\boldsymbol{r}}_{S_c/B}]\boldsymbol{r}'_{S_c/B} - m_{\mathrm{S}}[\tilde{\boldsymbol{r}}_{S_c/B}][\tilde{\boldsymbol{\omega}}_{\mathcal{S}/\mathcal{B}}]\boldsymbol{r}'_{S_c/S} \\ &\quad - \boldsymbol{c}_\theta\left([I_{\mathrm{S},S_c}] - m_{\mathrm{S}}[\tilde{\boldsymbol{r}}_{S_c/B}][\tilde{\boldsymbol{r}}_{S_c/S}]\right)\hat{\boldsymbol{s}} \end{aligned} \tag{43}$$

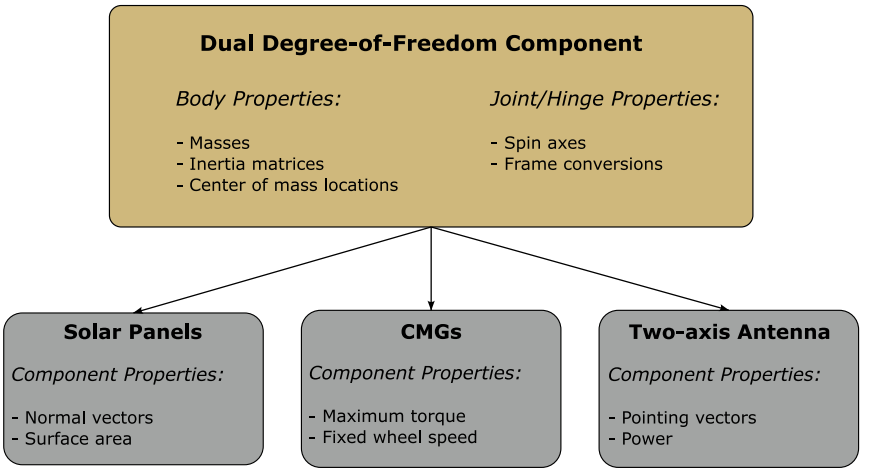

Fig. 4 Diagram for the two-axis rotating rigid-body class.

The Appendix shows the verification of the derived equations of motion by demonstrating that energy and angular momentum are conserved for the example problem.

IV. Dual-Axis Rotating Rigid-Body Dynamics

This section shows the derivation of the equations of motion of a dual-axis rotating rigid body attached to a rigid hub. The 2-DoF component can be described in one of two ways: first, as a chain of two rigid bodies connected by rotary joints, each rotating about a particular spin axis; second, as a single rigid body connected to the hub through a universal joint, which can have two spin axes. These descriptions can represent various common spacecraft components. Examples include dual-hinge solar arrays for deployment or second-order flexing analysis, control moment gyroscopes as attitude control devices, and two-axis gimbaled high-gain antennas. All these components can be defined through a general description, where they are specified by their masses, inertia matrices, location of the centers of mass, and spin axes. The module's implementation can be found here.[§§]

A diagram for the dual-axis rotating rigid-body class is shown in Fig. 4. It contains similar properties but is now adapted to represent a 2-DoF system. There are two masses, inertia matrices, center-of-mass locations, spin axes, and frame conversions. The equations of motion, mass properties, and energy and momentum contributions are adapted to dual-axis kinematics and dynamics.

Similar to the 1-DoF example, modules represented in gray follow from the 2-DoF parent structure. Examples include dual-hinged solar panels, control moment gyroscopes, and two-axis gimbaled antennas. As previously discussed, each module contains properties that define the specific component, such as a pointing vector for the antenna or a surface area for the solar panels.

An essential property of the dual-DoF formulation is that it can also represent a component connected through a dual-hinged joint. While the formulation takes two masses and two inertia tensors, it is possible to set the mass and inertia of the lower body to zero without introducing any singularity to the equations of motion. Instead of two bodies connected through rotary joints, the system represents a single body connected via a universal joint. This dramatically expands the configuration space to model using this formulation.

A. Problem Statement

The problem statement for the dual-axis rotating rigid body is illustrated in Fig. 5. The inertial frame is represented by $\mathcal{N}$ with origin at point N. The spacecraft comprises two rigid bodies connected to a rigid hub through two axes of rotation. The hub has a body-fixed frame $\mathcal{B}$ with origin B, and its center of mass is at point B_c. The mass of the hub is m_{hub}, and its inertia tensor about point B is $[I_{\text{hub},B}]$. The lower rotating rigid body has the $\mathcal{S}_1$ frame attached to it, originating at point S_1 and its center of mass at point S_{c_1}. The mass of the lower body is m_{S_1}, and its inertia tensor about its center of mass is $[I_{S_1,S_{c_1}}]$. The upper rotating rigid body has the $\mathcal{S}_2$ frame attached to it, originating at point S_2 and its center of mass at point S_{c_2}. The mass of the upper body is m_{S_2}, and its inertia tensor about its center of mass is $[I_{S_2,S_{c_2}}]$. The center of mass of the spinning system is located at point S_c, and its mass is m_S. The combined center of mass of the spacecraft is located at point C. The first spin axis $\hat{s}_1$ is constant, as seen by the $\mathcal{B}$ frame, and passes through the point S_1. The angle about this rotation axis is θ_1, and its angle rate is $\dot{\theta}_1$. The second spin axis $\hat{s}_2$ is constant, as seen by the $\mathcal{S}_1$ frame, and passes through the point S_2. The angle about this rotation axis is θ_2, and its angle rate is $\dot{\theta}_2$. Again, the position of points S_1 and S_2 do not change as seen from the $\mathcal{B}$ and $\mathcal{S}_1$ frames, respectively, since the axes of rotation pass through them.

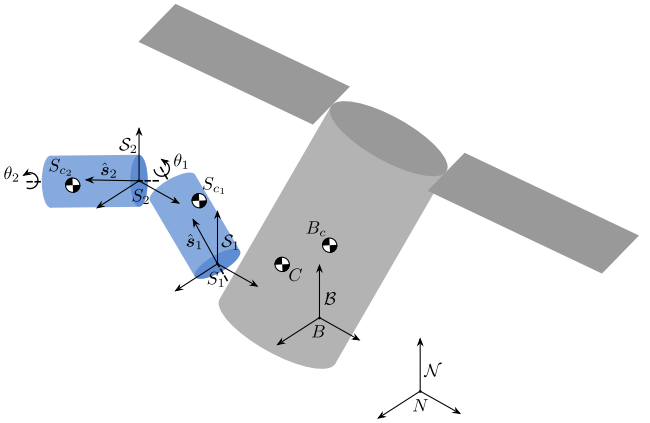

Fig. 5 Problem statement for the 2-DoF spinning rigid body.

The two-body description is used to describe the two-axis rotating rigid-body system as generally as possible. However, the resulting equations of motion still apply to a single rotating body attached by a universal joint. To do this, the mass and inertia tensor of the lower body are set to zero, which does not impart any singularity in the equations.

The dual-axis rotating rigid body attached to the hub has 8 degrees of freedom shown in Table 2: three for the system's position, three for the system's attitude, and one for the angle about each rotation axis. Like the 1-DoF case, the motion equations are developed to describe all 8 degrees of freedom. Therefore, beyond the translational and

[§§]Data available online at https://hanspeterschaub.info/basilisk/Documentation/simulation/dynamics/spinningBodies/spinningBodiesTwoDOF/spinningBodyTwoDOFStateEffector.html.

Table 2 State variables for the dual-axis rotating rigid-body spacecraft

State variables	Degrees of freedom	Equations of motion
$\boldsymbol{r}_{B/N}, \dot{\boldsymbol{r}}_{B/N}$	3	Translational
$\boldsymbol{\sigma}_{\mathcal{B}/\mathcal{N}}, \boldsymbol{\omega}_{\mathcal{B}/\mathcal{N}}$	3	Rotational
$\theta_1, \dot{\theta}_1$	1	First spinner rotational
$\theta_2, \dot{\theta}_2$	1	Second spinner rotational

rotational equations of motion, the system needs two spinner equations to describe each angle.

B. Translational Equations of Motion

For the translational equations of motion, the entire spacecraft is considered. This describes 3 degrees of freedom. Using the super particle theorem

$$m_{\mathrm{sc}}\ddot{\boldsymbol{r}}_{C/N} = m_{\mathrm{sc}}\ddot{\boldsymbol{r}}_{B/N} + m_{\mathrm{sc}}\ddot{\boldsymbol{c}} = \boldsymbol{F}_{\mathrm{ext}} \tag{44}$$

where $\boldsymbol{c} \equiv \boldsymbol{r}_{C/B}$. Using the definition of the center of mass of the system

$$m_{\mathrm{sc}}\boldsymbol{c} = m_{\mathrm{hub}}\boldsymbol{r}_{B_c/B} + m_{\mathrm{S}_1}\boldsymbol{r}_{S_{c_1}/B} + m_{\mathrm{S}_2}\boldsymbol{r}_{S_{c_2}/B} \tag{45}$$

and using the transport theorem, the inertial time derivatives can be expressed using body-frame derivatives as

$$\dot{\boldsymbol{c}} = \boldsymbol{c}' + \boldsymbol{\omega}_{\mathcal{B}/\mathcal{N}} \times \boldsymbol{c} \tag{46}$$

$$\ddot{\boldsymbol{c}} = \boldsymbol{c}'' + \dot{\boldsymbol{\omega}}_{\mathcal{B}/\mathcal{N}} \times \boldsymbol{c} + 2\boldsymbol{\omega}_{\mathcal{B}/\mathcal{N}} \times \boldsymbol{c}' + \boldsymbol{\omega}_{\mathcal{B}/\mathcal{N}} \times (\boldsymbol{\omega}_{\mathcal{B}/\mathcal{N}} \times \boldsymbol{c}) \tag{47}$$

The first-order body-frame derivatives for the three terms that are part of $\boldsymbol{c}$ are given by

$$\boldsymbol{r}'_{B_c/B} = \boldsymbol{0} \tag{48}$$

$$\boldsymbol{r}'_{S_{c_1}/B} = \boldsymbol{r}'_{S_{c_1}/S_1} = \boldsymbol{\omega}_{\mathcal{S}_1/\mathcal{B}} \times \boldsymbol{r}_{S_{c_1}/S_1} \tag{49}$$

$$\boldsymbol{r}'_{S_{c_2}/B} = \boldsymbol{r}'_{S_{c_2}/S_2} + \boldsymbol{r}'_{S_2/S_1} = \boldsymbol{\omega}_{\mathcal{S}_2/\mathcal{B}} \times \boldsymbol{r}_{S_{c_2}/S_2} + \boldsymbol{\omega}_{\mathcal{S}_1/\mathcal{B}} \times \boldsymbol{r}_{S_2/S_1} \tag{50}$$

where, by definition, $\boldsymbol{\omega}_{\mathcal{S}_1/\mathcal{B}} = \dot{\theta}_1\hat{\boldsymbol{s}}_1$ and $\boldsymbol{\omega}_{\mathcal{S}_2/\mathcal{B}} = \boldsymbol{\omega}_{\mathcal{S}_2/\mathcal{S}_1} + \boldsymbol{\omega}_{\mathcal{S}_1/\mathcal{B}} = \dot{\theta}_2\hat{\boldsymbol{s}}_2 + \dot{\theta}_1\hat{\boldsymbol{s}}_1$. In the equation above, some terms vanish because $\boldsymbol{r}_{S_1/B}$ and $\boldsymbol{r}_{S_2/S_1}$ are constant as seen from the $\mathcal{B}$ and $\mathcal{S}_1$ frames, respectively, because the spin axes pass through points S_1 and S_2. The second-order body-frame derivatives are given by

$$\boldsymbol{r}''_{B_c/B} = \boldsymbol{0} \tag{51}$$

$$\boldsymbol{r}''_{S_{c_1}/B} = \ddot{\theta}_1\hat{\boldsymbol{s}}_1 \times \boldsymbol{r}_{S_{c_1}/S_1} + \boldsymbol{\omega}_{\mathcal{S}_1/\mathcal{B}} \times \boldsymbol{r}'_{S_{c_1}/S_1} \tag{52}$$

$$\begin{aligned}\boldsymbol{r}''_{S_{c_2}/B} = {} & \ddot{\theta}_2\hat{\boldsymbol{s}}_2 \times \boldsymbol{r}_{S_{c_2}/S_2} + \ddot{\theta}_1\hat{\boldsymbol{s}}_1 \times \boldsymbol{r}_{S_{c_2}/S_1} + \left(\boldsymbol{\omega}_{\mathcal{S}_1/\mathcal{B}} \times \boldsymbol{\omega}_{\mathcal{S}_2/\mathcal{S}_1}\right) \times \boldsymbol{r}_{S_{c_2}/S_2} \\ & + \boldsymbol{\omega}_{\mathcal{S}_2/\mathcal{S}_1} \times \boldsymbol{r}'_{S_{c_2}/S_2} + \boldsymbol{\omega}_{\mathcal{S}_1/\mathcal{B}} \times \boldsymbol{r}'_{S_{c_2}/S_1}\end{aligned} \tag{53}$$

where $\boldsymbol{\omega}'_{\mathcal{S}_1/\mathcal{B}} = \ddot{\theta}_1\hat{\boldsymbol{s}}_1$ and $\boldsymbol{\omega}'_{\mathcal{S}_2/\mathcal{B}} = \ddot{\theta}_1\hat{\boldsymbol{s}}_1 + \ddot{\theta}_2\hat{\boldsymbol{s}}_2 + \boldsymbol{\omega}_{\mathcal{S}_1/\mathcal{B}} \times \boldsymbol{\omega}_{\mathcal{S}_2/\mathcal{S}_1}$ because $\hat{\boldsymbol{s}}_1$ is fixed in the $\mathcal{B}$ frame and $\hat{\boldsymbol{s}}_2$ is fixed in the $\mathcal{S}_1$ frame. With these results, the expressions for $m_{\mathrm{sc}}\boldsymbol{c}'$ and $m_{\mathrm{sc}}\boldsymbol{c}''$ are

$$m_{\mathrm{sc}}\boldsymbol{c}' = m_{\mathrm{S}_1}\boldsymbol{r}'_{S_{c_1}/B} + m_{\mathrm{S}_2}\boldsymbol{r}'_{S_{c_2}/B} = m_{\mathrm{S}}\boldsymbol{r}'_{S_c/B} \tag{54}$$

$$\begin{aligned}m_{\mathrm{sc}}\boldsymbol{c}'' = {} & m_{\mathrm{S}_1}\boldsymbol{r}''_{S_{c_1}/B} + m_{\mathrm{S}_2}\boldsymbol{r}''_{S_{c_2}/B} \\ = {} & -m_{\mathrm{S}}[\tilde{\boldsymbol{r}}_{S_c/S_1}]\hat{\boldsymbol{s}}_1\ddot{\theta}_1 - m_{\mathrm{S}_2}[\tilde{\boldsymbol{r}}_{S_{c_2}/S_2}]\hat{\boldsymbol{s}}_2\ddot{\theta}_2 + m_{\mathrm{S}}[\tilde{\boldsymbol{\omega}}_{\mathcal{S}_1/\mathcal{B}}]\boldsymbol{r}'_{S_c/B} \\ & + m_{\mathrm{S}_2}\left([\tilde{\boldsymbol{\omega}}_{\mathcal{S}_2/\mathcal{S}_1}]\boldsymbol{r}'_{S_{c_2}/S_2} - [\tilde{\boldsymbol{r}}_{S_{c_2}/S_2}][\tilde{\boldsymbol{\omega}}_{\mathcal{S}_1/\mathcal{B}}]\boldsymbol{\omega}_{\mathcal{S}_2/\mathcal{S}_1}\right)\end{aligned} \tag{55}$$

The center of mass of the spinning bodies system about point S_1 is defined as $m_{\mathrm{S}}\boldsymbol{r}_{S_c/S_1} = m_{S_1}\boldsymbol{r}_{S_{c_1}/S_1} + m_{S_2}\boldsymbol{r}_{S_{c_2}/S1}$. Finally, combining similar terms yields

$$\begin{aligned}& m_{\mathrm{sc}}\ddot{\boldsymbol{r}}_{\mathcal{B}/\mathcal{N}} - m_{\mathrm{sc}}[\tilde{\boldsymbol{c}}]\dot{\boldsymbol{\omega}}_{\mathcal{B}/\mathcal{N}} - m_{\mathrm{S}}[\tilde{\boldsymbol{r}}_{S_c/S_1}]\hat{\boldsymbol{s}}_1\ddot{\theta}_1 - m_{\mathrm{S}_2}[\tilde{\boldsymbol{r}}_{S_{c_2}/S_2}]\hat{\boldsymbol{s}}_2\ddot{\theta}_2 \\ & \quad = \boldsymbol{F}_{\mathrm{ext}} - 2m_{\mathrm{sc}}[\tilde{\boldsymbol{\omega}}_{\mathcal{B}/\mathcal{N}}]\boldsymbol{c}' - m_{\mathrm{sc}}[\tilde{\boldsymbol{\omega}}_{\mathcal{B}/\mathcal{N}}][\tilde{\boldsymbol{\omega}}_{\mathcal{B}/\mathcal{N}}]\boldsymbol{c} - m_{\mathrm{S}}[\tilde{\boldsymbol{\omega}}_{\mathcal{S}_1/\mathcal{B}}]\boldsymbol{r}'_{S_c/B} \\ & \quad - m_{\mathrm{S}_2}\left([\tilde{\boldsymbol{\omega}}_{\mathcal{S}_2/\mathcal{S}_1}]\boldsymbol{r}'_{S_{c_2}/S_2} - [\tilde{\boldsymbol{r}}_{S_{c_2}/S_2}][\tilde{\boldsymbol{\omega}}_{\mathcal{S}_1/\mathcal{B}}]\boldsymbol{\omega}_{\mathcal{S}_2/\mathcal{S}_1}\right)\end{aligned} \tag{56}$$

C. Rotational Equations of Motion

For the rotational equation of motion, the entire spacecraft is considered. This equation of motion describes the 3 degrees of freedom of the system. The rotational differential equation given about point B, which is not the system's center of mass, is given by

$$\dot{\boldsymbol{H}}_{\mathrm{sc},B} = \boldsymbol{L}_B + m_{\mathrm{sc}}\ddot{\boldsymbol{r}}_{B/N} \times \boldsymbol{c} \tag{57}$$

The angular momentum about point B is

$$\begin{aligned}\boldsymbol{H}_{\mathrm{sc},B} = {} & \boldsymbol{H}_{\mathrm{hub},B} + \boldsymbol{H}_{S_1,B} + \boldsymbol{H}_{S_2,B} \\ = {} & [I_{\mathrm{hub},B}]\boldsymbol{\omega}_{\mathcal{B}/\mathcal{N}} + [I_{S_1,S_{c_1}}]\boldsymbol{\omega}_{\mathcal{S}_1/\mathcal{N}} + m_{S_1}\boldsymbol{r}_{S_{c_1}/B} \times \dot{\boldsymbol{r}}_{S_{c_1}/B} \\ & + [I_{S_2,S_{c_2}}]\boldsymbol{\omega}_{\mathcal{S}_2/\mathcal{N}} + m_{S_2}\boldsymbol{r}_{S_{c_2}/B} \times \dot{\boldsymbol{r}}_{S_{c_2}/B}\end{aligned} \tag{58}$$

As previously discussed, it is useful to express the inertial time derivative using the $\mathcal{B}$ frame derivative and the transport theorem by noting that $\boldsymbol{\omega}_{\mathcal{S}_1/\mathcal{N}} = \boldsymbol{\omega}_{\mathcal{S}_1/\mathcal{B}} + \boldsymbol{\omega}_{\mathcal{B}/\mathcal{N}}$ and $\dot{\boldsymbol{r}}_{S_{c_1}/B} = \boldsymbol{r}'_{S_{c_1}/B} + \boldsymbol{\omega}_{\mathcal{B}/\mathcal{N}} \times \boldsymbol{r}_{S_{c_1}/B}$. An equivalent development can be used for the second spinning body. Grouping the terms multiplied by each angular velocity yields

$$\begin{aligned}\boldsymbol{H}_{\mathrm{sc},B} = {} & [I_{\mathrm{sc},B}]\boldsymbol{\omega}_{\mathcal{B}/\mathcal{N}} + [I_{S_1,S_{c_1}}]\boldsymbol{\omega}_{\mathcal{S}_1/\mathcal{B}} + [I_{S_2,S_{c_2}}]\boldsymbol{\omega}_{\mathcal{S}_2/\mathcal{B}} \\ & + m_{S_1}\boldsymbol{r}_{S_{c_1}/B} \times \boldsymbol{r}'_{S_{c_1}/B} + m_{S_2}\boldsymbol{r}_{S_{c_2}/B} \times \boldsymbol{r}'_{S_{c_2}/B}\end{aligned} \tag{59}$$

where $[I_{\mathrm{sc},B}] = [I_{\mathrm{hub},B}] + [I_{S_1,S_{c_1}}] + [I_{S_2,S_{c_2}}] - m_{S_1}[\tilde{\boldsymbol{r}}_{S_{c_1}/B}][\tilde{\boldsymbol{r}}_{S_{c_1}/B}] - m_{S_2}[\tilde{\boldsymbol{r}}_{S_{c_2}/B}][\tilde{\boldsymbol{r}}_{S_{c_2}/B}]$ is the spacecraft's total inertia about point B. To take the inertial time derivative of the total angular momentum, the transport theorem is used to take the body-frame time derivatives instead, which yields

$$\dot{\boldsymbol{H}}_{\mathrm{sc},B} = \boldsymbol{H}'_{\mathrm{sc},B} + \boldsymbol{\omega}_{\mathcal{B}/\mathcal{N}} \times \boldsymbol{H}_{\mathrm{sc},B} \tag{60}$$

The body-frame derivative of the angular momentum is

$$\begin{aligned}\boldsymbol{H}'_{\mathrm{sc},B} = {} & [I'_{\mathrm{sc},B}]\boldsymbol{\omega}_{\mathcal{B}/\mathcal{N}} + [I_{\mathrm{sc},B}]\dot{\boldsymbol{\omega}}_{\mathcal{B}/\mathcal{N}} + [I'_{S_1,S_{c_1}}]\boldsymbol{\omega}_{\mathcal{S}_1/\mathcal{B}} + [I_{S_1,S_{c_1}}]\boldsymbol{\omega}'_{\mathcal{S}_1/\mathcal{B}} \\ & + [I'_{S_2,S_{c_2}}]\boldsymbol{\omega}_{\mathcal{S}_2/\mathcal{B}} + [I_{S_2,S_{c_2}}]\boldsymbol{\omega}'_{\mathcal{S}_2/\mathcal{B}} + m_{S_1}\boldsymbol{r}_{S_{c_1}/B} \times \boldsymbol{r}''_{S_{c_1}/B} \\ & + m_{S_2}\boldsymbol{r}_{S_{c_2}/B} \times \boldsymbol{r}''_{S_{c_2}/B}\end{aligned} \tag{61}$$

where the derivative product rule is applied. To simplify the expression above, the body-frame derivatives of the inertia tensors are defined using the inertia transport theorem

$$[I'_{S_1,S_{c_1}}] = [\tilde{\boldsymbol{\omega}}_{\mathcal{S}_1/\mathcal{B}}][I_{S_1,S_{c_1}}] - [I_{S_1,S_{c_1}}][\tilde{\boldsymbol{\omega}}_{\mathcal{S}_1/\mathcal{B}}] \tag{62}$$

$$[I'_{S_2,S_{c_2}}] = [\tilde{\boldsymbol{\omega}}_{\mathcal{S}_2/\mathcal{B}}][I_{S_2,S_{c_2}}] - [I_{S_2,S_{c_2}}][\tilde{\boldsymbol{\omega}}_{\mathcal{S}_2/\mathcal{B}}] \tag{63}$$

$$[I'_{\mathrm{sc},B}] = [I'_{S_1,S_{c_1}}] + [I'_{S_2,S_{c_2}}] - m_{S_1}\left([\tilde{\boldsymbol{r}}'_{S_{c_1}/B}][\tilde{\boldsymbol{r}}_{S_{c_1}/B}] + [\tilde{\boldsymbol{r}}_{S_{c_1}/B}][\tilde{\boldsymbol{r}}'_{S_{c_1}/B}]\right) - m_{S_2}\left([\tilde{\boldsymbol{r}}'_{S_{c_2}/B}][\tilde{\boldsymbol{r}}_{S_{c_2}/B}] + [\tilde{\boldsymbol{r}}_{S_{c_2}/B}][\tilde{\boldsymbol{r}}'_{S_{c_2}/B}]\right) \tag{64}$$

Combining these results with the definitions derived in the translational equation of motion sections yields the following rotational equation of motion

$$\begin{aligned}
&m_{\mathrm{sc}}[\tilde{\boldsymbol{c}}]\ddot{\boldsymbol{r}}_{\mathcal{B}/\mathcal{N}} + [I_{\mathrm{sc},B}]\dot{\boldsymbol{\omega}}_{\mathcal{B}/\mathcal{N}} + \Big([I_{\mathrm{S}_1,S_{c_1}}] + [I_{\mathrm{S}_2,S_{c_2}}] \\
&\quad - m_{\mathrm{S}_1}[\tilde{\boldsymbol{r}}_{S_{c_1}/B}][\tilde{\boldsymbol{r}}_{S_{c_1}/S_1}] - m_{\mathrm{S}_2}[\tilde{\boldsymbol{r}}_{S_{c_2}/B}][\tilde{\boldsymbol{r}}_{S_{c_2}/S_1}]\Big)\hat{\boldsymbol{s}}_1\ddot{\theta}_1 \\
&\quad + \Big([I_{\mathrm{S}_2,S_{c_2}}] - m_{\mathrm{S}_2}[\tilde{\boldsymbol{r}}_{S_{c_2}/B}][\tilde{\boldsymbol{r}}_{S_{c_2}/S_2}]\Big)\hat{\boldsymbol{s}}_2\ddot{\theta}_2 \\
&\quad = \boldsymbol{L}_B - \Big([I'_{\mathrm{sc},B}] + [\tilde{\boldsymbol{\omega}}_{\mathcal{B}/\mathcal{N}}][I_{\mathrm{sc},B}]\Big)\boldsymbol{\omega}_{\mathcal{B}/\mathcal{N}} \\
&\quad - \Big([I'_{\mathrm{S}_1,S_{c_1}}] + [\tilde{\boldsymbol{\omega}}_{\mathcal{B}/\mathcal{N}}][I_{\mathrm{S}_1,S_{c_1}}]\Big)\boldsymbol{\omega}_{\mathcal{S}_1/\mathcal{B}} \\
&\quad - \Big([I'_{\mathrm{S}_2,S_{c_2}}] + [\tilde{\boldsymbol{\omega}}_{\mathcal{B}/\mathcal{N}}][I_{\mathrm{S}_2,S_{c_2}}]\Big)\boldsymbol{\omega}_{\mathcal{S}_2/\mathcal{B}} \\
&\quad - \Big([I_{\mathrm{S}_2,S_{c_2}}] - m_{\mathrm{S}_2}[\tilde{\boldsymbol{r}}_{S_{c_2}/B}][\tilde{\boldsymbol{r}}_{S_{c_2}/S_2}]\Big)[\tilde{\boldsymbol{\omega}}_{\mathcal{S}_1/\mathcal{B}}]\boldsymbol{\omega}_{\mathcal{S}_2/\mathcal{S}_1} \\
&\quad - m_{\mathrm{S}_1}\Big([\tilde{\boldsymbol{r}}_{S_{c_1}/B}][\tilde{\boldsymbol{\omega}}_{\mathcal{S}_1/\mathcal{B}}] + [\tilde{\boldsymbol{\omega}}_{\mathcal{B}/\mathcal{N}}][\tilde{\boldsymbol{r}}_{S_{c_1}/B}]\Big)\boldsymbol{r}'_{S_{c_1}/B} \\
&\quad - m_{\mathrm{S}_2}\Big([\tilde{\boldsymbol{r}}_{S_{c_2}/B}][\tilde{\boldsymbol{\omega}}_{\mathcal{S}_1/\mathcal{B}}] + [\tilde{\boldsymbol{\omega}}_{\mathcal{B}/\mathcal{N}}][\tilde{\boldsymbol{r}}_{S_{c_2}/B}]\Big)\boldsymbol{r}'_{S_{c_2}/B} \\
&\quad - m_{\mathrm{S}_2}[\tilde{\boldsymbol{r}}_{S_{c_2}/B}][\tilde{\boldsymbol{\omega}}_{\mathcal{S}_2/\mathcal{S}_1}]\boldsymbol{r}'_{S_{c_2}/S_2}
\end{aligned} \tag{65}$$

D. First Spinning Body Equations of Motion

The first spinning body equation of motion describes the motion of the spinning body system, defining another DoF of the spacecraft. The formulation of the equation of motion for the spinning body system is

$$\dot{\boldsymbol{H}}_{S,S_1} = \boldsymbol{L}_{S_1} - m_{\mathrm{S}}\boldsymbol{r}_{S_c/S_1} \times \ddot{\boldsymbol{r}}_{S_1/N} \tag{66}$$

The angular momentum of the spinning system is

$$\begin{aligned}
\boldsymbol{H}_{S,S_1} &= \boldsymbol{H}_{S_1,S_1} + \boldsymbol{H}_{S_2,S_1} \\
&= [I_{S_1,S_{c_1}}]\boldsymbol{\omega}_{\mathcal{S}_1/\mathcal{N}} + m_{S_1}\boldsymbol{r}_{S_{c_1}/S_1} \times \dot{\boldsymbol{r}}_{S_{c_1}/S_1} + [I_{S_2,S_{c_2}}]\boldsymbol{\omega}_{\mathcal{S}_2/\mathcal{N}} \\
&\quad + m_{S_2}\boldsymbol{r}_{S_{c_2}/S_1} \times \dot{\boldsymbol{r}}_{S_{c_2}/S_1}
\end{aligned} \tag{67}$$

The expression above can be simplified by applying the transport theorem to the $\dot{\boldsymbol{r}}$ terms and grouping the $\boldsymbol{\omega}_{\mathcal{B}/\mathcal{N}}$ terms as follows:

$$\begin{aligned}
\boldsymbol{H}_{S,S_1} &= [I_{\mathrm{S},S_1}]\boldsymbol{\omega}_{\mathcal{B}/\mathcal{N}} + [I_{S_1,S_{c_1}}]\boldsymbol{\omega}_{\mathcal{S}_1/\mathcal{B}} + [I_{S_2,S_{c_2}}]\boldsymbol{\omega}_{\mathcal{S}_2/\mathcal{B}} \\
&\quad + m_{S_1}\boldsymbol{r}_{S_{c_1}/S_1} \times \boldsymbol{r}'_{S_{c_1}/S_1} + m_{S_2}\boldsymbol{r}_{S_{c_2}/S_1} \times \boldsymbol{r}'_{S_{c_2}/S_1}
\end{aligned} \tag{68}$$

where three new inertia tensors are defined

$$[I_{\mathrm{S},S_1}] = [I_{S_1,S_1}] + [I_{S_2,S_1}] \tag{69}$$

$$[I_{S_1,S_1}] = [I_{S_1,S_{c_1}}] - m_{S_1}[\tilde{\boldsymbol{r}}_{S_{c_1}/S_1}][\tilde{\boldsymbol{r}}_{S_{c_1}/S_1}] \tag{70}$$

$$[I_{S_2,S_1}] = [I_{S_2,S_{c_2}}] - m_{S_2}[\tilde{\boldsymbol{r}}_{S_{c_2}/S_1}][\tilde{\boldsymbol{r}}_{S_{c_2}/S_1}] \tag{71}$$

Using the transport theorem to take the derivatives in the $\mathcal{B}$ frame, the inertial time derivative of the angular momentum is given by

$$\dot{\boldsymbol{H}}_{S,S_1} = \boldsymbol{H}'_{S,S_1} + \boldsymbol{\omega}_{\mathcal{B}/\mathcal{N}} \times \boldsymbol{H}_{S,S_1} \tag{72}$$

The body-frame derivative of the angular momentum is

$$\begin{aligned}
\boldsymbol{H}'_{S,S_1} &= [I'_{\mathrm{S},S_1}]\boldsymbol{\omega}_{\mathcal{B}/\mathcal{N}} + [I_{\mathrm{S},S_1}]\dot{\boldsymbol{\omega}}_{\mathcal{B}/\mathcal{N}} + [I'_{S_1,S_{c_1}}]\boldsymbol{\omega}_{\mathcal{S}_1/\mathcal{B}} + [I_{S_1,S_{c_1}}]\boldsymbol{\omega}'_{\mathcal{S}_1/\mathcal{B}} \\
&\quad + [I'_{S_2,S_{c_2}}]\boldsymbol{\omega}_{\mathcal{S}_2/\mathcal{B}} + [I_{S_2,S_{c_2}}]\boldsymbol{\omega}'_{\mathcal{S}_2/\mathcal{B}} + m_{S_1}\boldsymbol{r}_{S_{c_1}/S_1} \times \boldsymbol{r}''_{S_{c_1}/S_1} \\
&\quad + m_{S_2}\boldsymbol{r}_{S_{c_2}/S_1} \times \boldsymbol{r}''_{S_{c_2}/S_1}
\end{aligned} \tag{73}$$

The body-frame derivatives of the inertia tensors are

$$[I'_{\mathrm{S},S_1}] = [I'_{S_1,S_1}] + [I'_{S_2,S_1}] \tag{74}$$

$$[I'_{S_1,S_1}] = [I'_{S_1,S_{c_1}}] - m_{S_1}\left([\tilde{\boldsymbol{r}}'_{S_{c_1}/S_1}][\tilde{\boldsymbol{r}}_{S_{c_1}/S_1}] + [\tilde{\boldsymbol{r}}_{S_{c_1}/S_1}][\tilde{\boldsymbol{r}}'_{S_{c_1}/S_1}]\right) \tag{75}$$

$$[I'_{S_2,S_1}] = [I'_{S_2,S_{c_2}}] - m_{S_2}\left([\tilde{\boldsymbol{r}}'_{S_{c_2}/S_1}][\tilde{\boldsymbol{r}}_{S_{c_2}/S_1}] + [\tilde{\boldsymbol{r}}_{S_{c_2}/S_1}][\tilde{\boldsymbol{r}}'_{S_{c_2}/S_1}]\right) \tag{76}$$

As for the $\ddot{\boldsymbol{r}}_{S_1/N}$ term, it can be separated into two terms:

$$\ddot{\boldsymbol{r}}_{S_1/N} = \ddot{\boldsymbol{r}}_{S_1/B} + \ddot{\boldsymbol{r}}_{B/N} \tag{77}$$

To compute $\ddot{\boldsymbol{r}}_{S_1/B}$, it should be noted that $\boldsymbol{r}_{S_1/B}$ is constant in the $\mathcal{B}$ frame, which yields

$$\dot{\boldsymbol{r}}_{S_1/B} = \boldsymbol{\omega}_{\mathcal{B}/\mathcal{N}} \times \boldsymbol{r}_{S_1/B}, \quad \ddot{\boldsymbol{r}}_{S_1/B} = \dot{\boldsymbol{\omega}}_{\mathcal{B}/\mathcal{N}} \times \boldsymbol{r}_{S_1/B} + \boldsymbol{\omega}_{\mathcal{B}/\mathcal{N}} \times \dot{\boldsymbol{r}}_{S_1/B} \tag{78}$$

Here, all terms are dotted with the spin axis $\hat{\boldsymbol{s}}_1$ to ignore the dynamics in any other direction, where structural torques keep the constraints in place. This results in the first spinning body equation of motion:

$$\begin{aligned}
&\hat{\boldsymbol{s}}_1^T[I_{\mathrm{S},S_1}]\hat{\boldsymbol{s}}_1\ddot{\theta}_1 + \hat{\boldsymbol{s}}_1^T\Big([I_{S_2,S_{c_2}}] - m_{S_2}[\tilde{\boldsymbol{r}}_{S_{c_2}/S_1}][\tilde{\boldsymbol{r}}_{S_{c_2}/S_2}]\Big)\hat{\boldsymbol{s}}_2\ddot{\theta}_2 \\
&\quad = u_{S_1} - m_{\mathrm{S}}\hat{\boldsymbol{s}}_1^T[\tilde{\boldsymbol{r}}_{S_c/S_1}]\ddot{\boldsymbol{r}}_{B/N} - \hat{\boldsymbol{s}}_1^T\Big([I_{\mathrm{S},S_1}] - m_{\mathrm{S}}[\tilde{\boldsymbol{r}}_{S_c/S_1}][\tilde{\boldsymbol{r}}_{S_1/B}]\Big)\dot{\boldsymbol{\omega}}_{\mathcal{B}/\mathcal{N}} \\
&\quad - \hat{\boldsymbol{s}}_1^T\Big([I'_{\mathrm{S},S_1}] + [\tilde{\boldsymbol{\omega}}_{\mathcal{B}/\mathcal{N}}][I_{\mathrm{S},S_1}]\Big)\boldsymbol{\omega}_{\mathcal{B}/\mathcal{N}} \\
&\quad - \hat{\boldsymbol{s}}_1^T\Big([I'_{S_1,S_{c_1}}] + [\tilde{\boldsymbol{\omega}}_{\mathcal{B}/\mathcal{N}}][I_{S_1,S_{c_1}}]\Big)\boldsymbol{\omega}_{\mathcal{S}_1/\mathcal{B}} \\
&\quad - \hat{\boldsymbol{s}}_1^T\Big([I'_{S_2,S_{c_2}}] + [\tilde{\boldsymbol{\omega}}_{\mathcal{B}/\mathcal{N}}][I_{S_2,S_{c_2}}]\Big)\boldsymbol{\omega}_{\mathcal{S}_2/\mathcal{B}} \\
&\quad - \hat{\boldsymbol{s}}_1^T\Big([I_{S_2,S_{c_2}}] - m_{S_2}[\tilde{\boldsymbol{r}}_{S_{c_2}/S_1}][\tilde{\boldsymbol{r}}_{S_{c_2}/S_2}]\Big)[\tilde{\boldsymbol{\omega}}_{\mathcal{S}_1/\mathcal{B}}]\boldsymbol{\omega}_{\mathcal{S}_2/\mathcal{S}_1} \\
&\quad - m_{S_1}\hat{\boldsymbol{s}}_1^T\Big([\tilde{\boldsymbol{r}}_{S_{c_1}/S_1}][\tilde{\boldsymbol{\omega}}_{\mathcal{S}_1/\mathcal{B}}] + [\tilde{\boldsymbol{\omega}}_{\mathcal{B}/\mathcal{N}}][\tilde{\boldsymbol{r}}_{S_{c_1}/S_1}]\Big)\boldsymbol{r}'_{S_{c_1}/S_1} \\
&\quad - m_{S_2}\hat{\boldsymbol{s}}_1^T\Big([\tilde{\boldsymbol{r}}_{S_{c_2}/S_1}][\tilde{\boldsymbol{\omega}}_{\mathcal{S}_1/\mathcal{B}}] + [\tilde{\boldsymbol{\omega}}_{\mathcal{B}/\mathcal{N}}][\tilde{\boldsymbol{r}}_{S_{c_2}/S_1}]\Big)\boldsymbol{r}'_{S_{c_2}/S_1} \\
&\quad - m_{S_2}\hat{\boldsymbol{s}}_1^T[\tilde{\boldsymbol{r}}_{S_{c_2}/S_1}][\tilde{\boldsymbol{\omega}}_{\mathcal{S}_2/\mathcal{S}_1}]\boldsymbol{r}'_{S_{c_2}/S_2} - m_{\mathrm{S}}\hat{\boldsymbol{s}}_1^T[\tilde{\boldsymbol{r}}_{S_c/S_1}][\tilde{\boldsymbol{\omega}}_{\mathcal{B}/\mathcal{N}}]\dot{\boldsymbol{r}}_{S_1/B}
\end{aligned} \tag{79}$$

E. Second Spinning Body Equations of Motion

For the final equation of motion, only the top spinner is considered, describing the last DoF of the system. The formulation for the equation of motion for the second spinner is

$$\dot{\boldsymbol{H}}_{S_2,S_2} = \boldsymbol{L}_{S_2} - m_{S_2}\boldsymbol{r}_{S_{c_2}/S_2} \times \ddot{\boldsymbol{r}}_{S_2/N} \tag{80}$$

The angular momentum of the top spinner about point S_2 is

$$\boldsymbol{H}_{S_2,S_2} = [I_{S_2,S_2}]\boldsymbol{\omega}_{\mathcal{S}_2/\mathcal{N}} = [I_{S_2,S_2}]\boldsymbol{\omega}_{\mathcal{B}/\mathcal{N}} + [I_{S_2,S_2}]\boldsymbol{\omega}_{\mathcal{S}_2/\mathcal{B}} \tag{81}$$

where $[I_{S_2,S_2}]$ is defined as $[I_{S_2,S_2}] = [I_{S_2,S_{c_2}}] - m_{S_2}[\tilde{\boldsymbol{r}}_{S_{c_2}/S_2}][\tilde{\boldsymbol{r}}_{S_{c_2}/S_2}]$ using the parallel axis theorem. The inertial time derivative of the angular momentum is given by

$$\dot{\boldsymbol{H}}_{S_2,S_2} = \boldsymbol{H}'_{S_2,S_2} + \boldsymbol{\omega}_{\mathcal{B}/\mathcal{N}} \times \boldsymbol{H}_{S_2,S_2} \tag{82}$$

The body-frame time derivative of $\boldsymbol{H}_{S_2,S_2}$ is

$$\boldsymbol{H}'_{S_2,S_2} = [I'_{S_2,S_2}]\boldsymbol{\omega}_{\mathcal{B}/\mathcal{N}} + [I_{S_2,S_2}]\dot{\boldsymbol{\omega}}_{\mathcal{B}/\mathcal{N}} + [I'_{S_2,S_2}]\boldsymbol{\omega}_{\mathcal{S}_2/\mathcal{B}} + [I_{S_2,S_2}]\boldsymbol{\omega}'_{\mathcal{S}_2/\mathcal{B}} \tag{83}$$

As for the $\ddot{\boldsymbol{r}}_{S_2/N}$ term, it can be separated into three terms

$$\ddot{\boldsymbol{r}}_{S_2/N} = \ddot{\boldsymbol{r}}_{S_2/S_1} + \ddot{\boldsymbol{r}}_{S_1/B} + \ddot{\boldsymbol{r}}_{B/N} \tag{84}$$

where $\ddot{\boldsymbol{r}}_{S_2/S_1}$ is equal to

$$\dot{\boldsymbol{r}}_{S_2/S_1} = \boldsymbol{r}'_{S_2/S_1} + \boldsymbol{\omega}_{\mathcal{B}/\mathcal{N}} \times \boldsymbol{r}_{S_2/S_1} \tag{85}$$

$$\ddot{\boldsymbol{r}}_{S_2/S_1} = \boldsymbol{r}''_{S_2/S_1} + \dot{\boldsymbol{\omega}}_{\mathcal{B}/\mathcal{N}} \times \boldsymbol{r}_{S_2/S_1} + \boldsymbol{\omega}_{\mathcal{B}/\mathcal{N}} \times \boldsymbol{r}'_{S_2/S_1} + \boldsymbol{\omega}_{\mathcal{B}/\mathcal{N}} \times \dot{\boldsymbol{r}}_{S_2/S_1} \tag{86}$$

These results can be combined into the second spinning body equation of motion by dotting each term with $\hat{\boldsymbol{s}}_2$

$$\begin{aligned}
&\hat{\boldsymbol{s}}_2^T\Big([I_{S_2,S_2}] - m_{S_2}[\tilde{\boldsymbol{r}}_{S_{c_2}/S_2}][\tilde{\boldsymbol{r}}_{S_2/S_1}]\Big)\hat{\boldsymbol{s}}_1\ddot{\theta}_1 + \hat{\boldsymbol{s}}_2^T[I_{S_2,S_2}]\hat{\boldsymbol{s}}_2\ddot{\theta}_2 \\
&= u_{S_2} - m_{S_2}\hat{\boldsymbol{s}}_2^T[\tilde{\boldsymbol{r}}_{S_{c_2}/S_2}]\ddot{\boldsymbol{r}}_{B/N} - \hat{\boldsymbol{s}}_2^T\Big([I_{S_2,S_2}] - m_{S_2}[\tilde{\boldsymbol{r}}_{S_{c_2}/S_2}][\tilde{\boldsymbol{r}}_{S_2/B}]\Big)\dot{\boldsymbol{\omega}}_{\mathcal{B}/\mathcal{N}} \\
&- \hat{\boldsymbol{s}}_2^T\Big([I'_{S_2,S_2}] + [\tilde{\boldsymbol{\omega}}_{\mathcal{B}/\mathcal{N}}][I_{S_2,S_2}]\Big)\boldsymbol{\omega}_{\mathcal{S}_2/\mathcal{N}} - \hat{\boldsymbol{s}}_2^T[I_{S_2,S_2}][\tilde{\boldsymbol{\omega}}_{\mathcal{S}_1/\mathcal{B}}]\boldsymbol{\omega}_{\mathcal{S}_2/\mathcal{S}_1} \\
&- m_{S_2}\hat{\boldsymbol{s}}_2^T[\tilde{\boldsymbol{r}}_{S_{c_2}/S_2}][\tilde{\boldsymbol{\omega}}_{\mathcal{S}_1/\mathcal{N}}]\boldsymbol{r}'_{S_2/S_1} - m_{S_2}\hat{\boldsymbol{s}}_2^T[\tilde{\boldsymbol{r}}_{S_{c_2}/S_2}][\tilde{\boldsymbol{\omega}}_{\mathcal{B}/\mathcal{N}}](\dot{\boldsymbol{r}}_{S_2/S_1} + \dot{\boldsymbol{r}}_{S_1/B})
\end{aligned} \tag{87}$$

F. Backsubstitution Formulation

To get a compact formulation for both equations, they are expressed in matrix form as such

$$[\boldsymbol{M}_\theta]\ddot{\boldsymbol{\theta}} = [\boldsymbol{A}^*_\theta]\ddot{\boldsymbol{r}}_{B/N} + [\boldsymbol{B}^*_\theta]\dot{\boldsymbol{\omega}}_{\mathcal{B}/\mathcal{N}} + [\boldsymbol{C}^*_\theta] \tag{88}$$

where the matrices above are defined as

$$[\boldsymbol{M}_\theta] = \begin{bmatrix} \hat{\boldsymbol{s}}_1^T[I_{S,S_1}]\hat{\boldsymbol{s}}_1 & \hat{\boldsymbol{s}}_1^T\Big([I_{S_2,S_{c_2}}] - m_{S_2}[\tilde{\boldsymbol{r}}_{S_{c_2}/S_1}][\tilde{\boldsymbol{r}}_{S_{c_2}/S_2}]\Big)\hat{\boldsymbol{s}}_2 \\ \hat{\boldsymbol{s}}_2^T\Big([I_{S_2,S_2}] - m_{S_2}[\tilde{\boldsymbol{r}}_{S_{c_2}/S_2}][\tilde{\boldsymbol{r}}_{S_2/S_1}]\Big)\hat{\boldsymbol{s}}_1 & \hat{\boldsymbol{s}}_2^T[I_{S_2,S_2}]\hat{\boldsymbol{s}}_2 \end{bmatrix} \tag{89}$$

$$[\boldsymbol{A}^*_\theta] = \begin{bmatrix} -m_S\hat{\boldsymbol{s}}_1^T[\tilde{\boldsymbol{r}}_{S_c/S_1}] \\ -m_{S_2}\hat{\boldsymbol{s}}_2^T[\tilde{\boldsymbol{r}}_{S_{c_2}/S_2}] \end{bmatrix} \tag{90}$$

$$[\boldsymbol{B}^*_\theta] = \begin{bmatrix} -\hat{\boldsymbol{s}}_1^T\Big([I_{S,S_1}] - m_S[\tilde{\boldsymbol{r}}_{S_c/S_1}][\tilde{\boldsymbol{r}}_{S_1/B}]\Big) \\ -\hat{\boldsymbol{s}}_2^T\Big([I_{S_2,S_2}] - m_{S_2}[\tilde{\boldsymbol{r}}_{S_{c_2}/S_2}][\tilde{\boldsymbol{r}}_{S_2/B}]\Big) \end{bmatrix} \tag{91}$$

$$[\boldsymbol{C}^*_\theta] = \begin{bmatrix} u_{S_1} - \hat{\boldsymbol{s}}_1^T\Big\{\Big([I'_{S,S_1}] + [\tilde{\boldsymbol{\omega}}_{\mathcal{B}/\mathcal{N}}][I_{S,S_1}]\Big)\boldsymbol{\omega}_{\mathcal{B}/\mathcal{N}} + \Big([I'_{S_1,S_{c_1}}] + [\tilde{\boldsymbol{\omega}}_{\mathcal{B}/\mathcal{N}}][I_{S_1,S_{c_1}}]\Big)\boldsymbol{\omega}_{\mathcal{S}_1/\mathcal{B}} \\ +\Big([I'_{S_2,S_{c_2}}] + [\tilde{\boldsymbol{\omega}}_{\mathcal{B}/\mathcal{N}}][I_{S_2,S_{c_2}}]\Big)\boldsymbol{\omega}_{\mathcal{S}_2/\mathcal{B}} \\ +\Big([I_{S_2,S_{c_2}}] - m_{S_2}[\tilde{\boldsymbol{r}}_{S_{c_2}/S_1}][\tilde{\boldsymbol{r}}_{S_{c_2}/S_2}]\Big)[\tilde{\boldsymbol{\omega}}_{\mathcal{S}_1/\mathcal{B}}]\boldsymbol{\omega}_{\mathcal{S}_2/\mathcal{S}_1} \\ +m_{S_1}\Big([\tilde{\boldsymbol{r}}_{S_{c_1}/S_1}][\tilde{\boldsymbol{\omega}}_{\mathcal{S}_1/\mathcal{B}}] + [\tilde{\boldsymbol{\omega}}_{\mathcal{B}/\mathcal{N}}][\tilde{\boldsymbol{r}}_{S_{c_1}/S_1}]\Big)\boldsymbol{r}'_{S_{c_1}/S_1} \\ +m_{S_2}\Big([\tilde{\boldsymbol{r}}_{S_{c_2}/S_1}][\tilde{\boldsymbol{\omega}}_{\mathcal{S}_1/\mathcal{B}}] + [\tilde{\boldsymbol{\omega}}_{\mathcal{B}/\mathcal{N}}][\tilde{\boldsymbol{r}}_{S_{c_2}/S_1}]\Big)\boldsymbol{r}'_{S_{c_2}/S_1} \\ +m_{S_2}[\tilde{\boldsymbol{r}}_{S_{c_2}/S_1}][\tilde{\boldsymbol{\omega}}_{\mathcal{S}_2/\mathcal{S}_1}]\boldsymbol{r}'_{S_{c_2}/S_2} + m_S[\tilde{\boldsymbol{r}}_{S_c/S_1}][\tilde{\boldsymbol{\omega}}_{\mathcal{B}/\mathcal{N}}]\dot{\boldsymbol{r}}_{S_1/B}\Big\} \\ \\ u_{S_2} - \hat{\boldsymbol{s}}_2^T\Big\{([I'_{S_2,S_2}] + [\tilde{\boldsymbol{\omega}}_{\mathcal{B}/\mathcal{N}}][I_{S_2,S_2}]\Big)\boldsymbol{\omega}_{\mathcal{S}_2/\mathcal{N}} + [I_{S_2,S_2}][\tilde{\boldsymbol{\omega}}_{\mathcal{S}_1/\mathcal{B}}]\boldsymbol{\omega}_{\mathcal{S}_2/\mathcal{S}_1} + \\ m_{S_2}[\tilde{\boldsymbol{r}}_{S_{c_2}/S_2}][\tilde{\boldsymbol{\omega}}_{\mathcal{S}_1/\mathcal{N}}]\boldsymbol{r}'_{S_2/S_1} + m_{S_2}[\tilde{\boldsymbol{r}}_{S_{c_2}/S_2}][\tilde{\boldsymbol{\omega}}_{\mathcal{B}/\mathcal{N}}]\Big(\dot{\boldsymbol{r}}_{S_2/S_1} + \dot{\boldsymbol{r}}_{S_1/B}\Big)\Big\} \end{bmatrix} \tag{92}$$

Note that the $[\boldsymbol{M}_\theta]$ matrix is full rank even when $m_{S_1} = 0$ and $[I_{S_1,S_1}] = \boldsymbol{0}$. This particular case represents a universal (two-axis) joint instead of the chain of rotary joints in the more general case. When the $[\boldsymbol{M}_\theta]$ matrix is inverted, no singularities appear due to its full rankness.

The canonical form of equation (88) is given by

$$\ddot{\boldsymbol{\theta}} = [\boldsymbol{A}_\theta]\ddot{\boldsymbol{r}}_{B/N} + [\boldsymbol{B}_\theta]\dot{\boldsymbol{\omega}}_{\mathcal{B}/\mathcal{N}} + [\boldsymbol{C}_\theta] \tag{93}$$

where the new matrices are defined as

$$[\boldsymbol{A}_\theta] = [\boldsymbol{M}_\theta]^{-1}[\boldsymbol{A}^*_\theta], \quad [\boldsymbol{B}_\theta] = [\boldsymbol{M}_\theta]^{-1}[\boldsymbol{B}^*_\theta], \quad [\boldsymbol{C}_\theta] = [\boldsymbol{M}_\theta]^{-1}[\boldsymbol{C}^*_\theta] \tag{94}$$

These results can be plugged into the backsubstitution formulation as such

$$\begin{bmatrix} [A] & [B] \\ [C] & [D] \end{bmatrix}\begin{bmatrix} \ddot{\boldsymbol{r}}_{B/N} \\ \dot{\boldsymbol{\omega}}_{\mathcal{B}/\mathcal{N}} \end{bmatrix} = \begin{bmatrix} \boldsymbol{v}_{\text{trans}} \\ \boldsymbol{v}_{\text{rot}} \end{bmatrix} \tag{95}$$

using the following matrices:

$$[A] = m_{sc}[I_{3\times3}] - m_S[\tilde{\boldsymbol{r}}_{S_c/S_1}]\hat{\boldsymbol{s}}_1\boldsymbol{A}_{\theta_1} - m_{S_2}[\tilde{\boldsymbol{r}}_{S_{c_2}/S_2}]\hat{\boldsymbol{s}}_2\boldsymbol{A}_{\theta_2} \tag{96}$$

$$[B] = -m_{sc}[\tilde{\boldsymbol{c}}] - m_S[\tilde{\boldsymbol{r}}_{S_c/S_1}]\hat{\boldsymbol{s}}_1\boldsymbol{B}_{\theta_1} - m_{S_2}[\tilde{\boldsymbol{r}}_{S_{c_2}/S_2}]\hat{\boldsymbol{s}}_2\boldsymbol{B}_{\theta_2} \tag{97}$$

$$\begin{aligned}
[C] = m_{sc}[\tilde{\boldsymbol{c}}] &+ \Big([I_{S_1,S_{c_1}}] + [I_{S_2,S_{c_2}}] - m_{S_1}[\tilde{\boldsymbol{r}}_{S_{c_1}/B}][\tilde{\boldsymbol{r}}_{S_{c_1}/S_1}] \\
&- m_{S_2}[\tilde{\boldsymbol{r}}_{S_{c_2}/B}][\tilde{\boldsymbol{r}}_{S_{c_2}/S_1}]\Big)\hat{\boldsymbol{s}}_1\boldsymbol{A}_{\theta_1} \\
&+ \Big([I_{S_2,S_{c_2}}] - m_{S_2}[\tilde{\boldsymbol{r}}_{S_{c_2}/B}][\tilde{\boldsymbol{r}}_{S_{c_2}/S_2}]\Big)\hat{\boldsymbol{s}}_2\boldsymbol{A}_{\theta_2}
\end{aligned} \tag{98}$$

$$[D] = [I_{\text{sc},B}] + \Big([I_{\text{S}_1,\mathcal{S}_{c_1}}] + [I_{\text{S}_2,\mathcal{S}_{c_2}}] - m_{\text{S}_1}[\tilde{\boldsymbol{r}}_{S_{c_1}/B}][\tilde{\boldsymbol{r}}_{S_{c_1}/S_1}] - m_{\text{S}_2}[\tilde{\boldsymbol{r}}_{S_{c_2}/B}][\tilde{\boldsymbol{r}}_{S_{c_2}/S_1}]\Big)\hat{\boldsymbol{s}}_1\boldsymbol{B}_{\theta_1} + \Big([I_{\text{S}_2,\mathcal{S}_{c_2}}] - m_{\text{S}_2}[\tilde{\boldsymbol{r}}_{S_{c_2}/B}][\tilde{\boldsymbol{r}}_{S_{c_2}/S_2}]\Big)\hat{\boldsymbol{s}}_2\boldsymbol{B}_{\theta_2} \tag{99}$$

and vectors

$$\boldsymbol{v}_{\text{trans}} = \boldsymbol{F}_{\text{ext}} - 2m_{\text{sc}}[\tilde{\boldsymbol{\omega}}_{\mathcal{B}/\mathcal{N}}]\boldsymbol{c}' - m_{\text{sc}}[\tilde{\boldsymbol{\omega}}_{\mathcal{B}/\mathcal{N}}][\tilde{\boldsymbol{\omega}}_{\mathcal{B}/\mathcal{N}}]\boldsymbol{c} - m_{\text{S}}[\tilde{\boldsymbol{\omega}}_{\mathcal{S}_1/\mathcal{B}}]\boldsymbol{r}'_{S_c/B} - m_{\text{S}_2}\Big([\tilde{\boldsymbol{\omega}}_{\mathcal{S}_2/\mathcal{S}_1}]\boldsymbol{r}'_{S_{c_2}/S_2} - [\tilde{\boldsymbol{r}}_{S_{c_2}/S_2}][\tilde{\boldsymbol{\omega}}_{\mathcal{S}_1/\mathcal{B}}]\boldsymbol{\omega}_{\mathcal{S}_2/\mathcal{S}_1}\Big) + m_{\text{S}}[\tilde{\boldsymbol{r}}_{S_c/S_1}]\hat{\boldsymbol{s}}_1\boldsymbol{C}_{\theta_1} + m_{\text{S}_2}[\tilde{\boldsymbol{r}}_{S_{c_2}/S_2}]\hat{\boldsymbol{s}}_2\boldsymbol{C}_{\theta_2} \tag{100}$$

$$\begin{aligned}\boldsymbol{v}_{\text{rot}} = {} & \boldsymbol{L}_B - [\tilde{\boldsymbol{\omega}}_{\mathcal{B}/\mathcal{N}}][I_{\text{sc},B}]\boldsymbol{\omega}_{\mathcal{B}/\mathcal{N}} - [I'_{\text{sc},B}]\boldsymbol{\omega}_{\mathcal{B}/\mathcal{N}} \\ & - \Big([I'_{S_{1},\mathcal{S}_{c_1}}] + [\tilde{\boldsymbol{\omega}}_{\mathcal{B}/\mathcal{N}}][I_{S_1,\mathcal{S}_{c_1}}]\Big)\boldsymbol{\omega}_{\mathcal{S}_1/\mathcal{B}} \\ & - \Big([I'_{S_{2},\mathcal{S}_{c_2}}] + [\tilde{\boldsymbol{\omega}}_{\mathcal{B}/\mathcal{N}}][I_{S_2,\mathcal{S}_{c_2}}]\Big)\boldsymbol{\omega}_{\mathcal{S}_2/\mathcal{B}} \\ & - \Big([I_{S_2,\mathcal{S}_{c_2}}] - m_{S_2}[\tilde{\boldsymbol{r}}_{S_{c_2}/B}][\tilde{\boldsymbol{r}}_{S_{c_2}/S_2}]\Big)[\tilde{\boldsymbol{\omega}}_{\mathcal{S}_1/\mathcal{B}}]\boldsymbol{\omega}_{\mathcal{S}_2/\mathcal{S}_1} \\ & - m_{S_1}\Big([\tilde{\boldsymbol{r}}_{S_{c_1}/B}][\tilde{\boldsymbol{\omega}}_{\mathcal{S}_1/\mathcal{B}}] + [\tilde{\boldsymbol{\omega}}_{\mathcal{B}/\mathcal{N}}][\tilde{\boldsymbol{r}}_{S_{c_1}/B}]\Big)\boldsymbol{r}'_{S_{c_1}/B} \\ & - m_{S_2}\Big([\tilde{\boldsymbol{r}}_{S_{c_2}/B}][\tilde{\boldsymbol{\omega}}_{\mathcal{S}_1/\mathcal{B}}] + [\tilde{\boldsymbol{\omega}}_{\mathcal{B}/\mathcal{N}}][\tilde{\boldsymbol{r}}_{S_{c_2}/B}]\Big)\boldsymbol{r}'_{S_{c_2}/B} \\ & - m_{S_2}[\tilde{\boldsymbol{r}}_{S_{c_2}/B}][\tilde{\boldsymbol{\omega}}_{\mathcal{S}_2/\mathcal{S}_1}]\boldsymbol{r}'_{S_{c_2}/S_2} - \Big([I_{S_1,\mathcal{S}_{c_1}}] + [I_{S_2,\mathcal{S}_{c_2}}] \\ & - m_{S_1}[\tilde{\boldsymbol{r}}_{S_{c_1}/B}][\tilde{\boldsymbol{r}}_{S_{c_1}/S_1}] - m_{S_2}[\tilde{\boldsymbol{r}}_{S_{c_2}/B}][\tilde{\boldsymbol{r}}_{S_{c_2}/S_1}]\Big)\hat{\boldsymbol{s}}_1\boldsymbol{C}_{\theta_1} \\ & - \Big([I_{S_2,\mathcal{S}_{c_2}}] - m_{S_2}[\tilde{\boldsymbol{r}}_{S_{c_2}/B}][\tilde{\boldsymbol{r}}_{S_{c_2}/S_2}]\Big)\hat{\boldsymbol{s}}_2\boldsymbol{C}_{\theta_2}\end{aligned} \tag{101}$$

The Appendix shows the verification of the derived equations of motion by demonstrating that energy and angular momentum are conserved for the example problem.

V. Numerical Simulation

This section describes a comprehensive simulation using the dual-axis component attached to a rigid hub. The software solution is implemented using the open-source Basilisk Astrodynamics Simulation Framework.[¶¶] The full spacecraft simulation scenario is found here.[***] The goals are to show the dynamic behavior of the components whose equations of motion have been given in previous sections and to demonstrate how a single implementation of the general model can describe an array of different components.

The hub comprises a solid cylinder with a diameter of 2 m and a height of 4 m. The mass and inertia properties of the spacecraft's hub are given in Table 3. The center of mass of the hub is assumed to coincide

Table 3 Simulation parameters for the rigid hub

Parameter	Notation	Value	Units
Hub's mass	m_{hub}	400	kg
Hub's inertia about the hub's center of mass	${}^{\mathcal{B}}[I_{\text{hub},B_c}]$	${}^{\mathcal{B}}\begin{bmatrix} 633.(3) & 0 & 0 \\ 0 & 633.(3) & 0 \\ 0 & 0 & 200 \end{bmatrix}$	kg · m^2
Hub's center-of-mass location with respect to B	${}^{\mathcal{B}}\boldsymbol{r}_{B_c/B}$	${}^{\mathcal{B}}[0,0,0]^T$	m

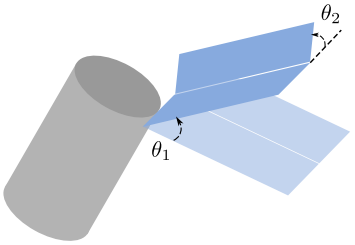

Fig. 6 Spacecraft with a hub and two panels in a parallel-hinge configuration. The figure shows two possible configurations: the translucent represents the undeflected state, while the opaque represents the deflected one.

with the origin of the body frame $\mathcal{B}$, a common assumption in dynamic systems. The initial attitude coincides with the inertial frame such that $\boldsymbol{\sigma}_{\mathcal{B}/\mathcal{N}} = [0,0,0]^T$, written in modified Rodrigues parameters, and the initial angular velocity is ${}^{\mathcal{B}}\boldsymbol{\omega}_{\mathcal{B}/\mathcal{N}} = [0.05, -0.05, 0.05]^T$ rad/s.

Two different simulations show the practicality and usefulness of having one general model. In the first simulation, a two-panel subsystem is added to the hub, as shown in Fig. 6. These panels are rectangular prisms with a length of 4 m, a width of 2 m, and a thickness of 0.1 m. The first panel connects to the hub by a rotary hinge (1 DoF), and the second connects to the first through another rotary hinge. The hinges are perpendicular to each other. This configuration represents a two-panel subsystem, which can be tucked in for launch and deployed once the spacecraft reaches orbit. The subsystem's properties for this specific simulation are shown in Table 4.

The time history for both θ angles and $\dot{\theta}$ angle rates is given in Figs. 7a and 7b. Overall, the angles are driven by the rotational spring and dampers introduced on each hinge. However, the cross-coupling between the two angles as the panels rotate is evident, especially when looking at the angle rates between 0 and 10 s. After that, both angles and angle rates are in phase with one another.

The time history for the hub's velocity and angular velocity are given in Figs. 8a and 8b. Here, two distinct phases are evident. At the beginning of the simulation, each component experiences a transient behavior that matches the oscillations shown in Fig. 7. This clearly shows the gyroscopic coupling between the panels and the rigid hub that is a direct consequence of the physics captured by the equations of motion shown before. Then, when the oscillations damp out, both the velocity and angular velocity stabilize into their steady-state behavior. Note that both the velocity and angular velocity settle with an oscillatory behavior, which is expected (even though no forces are present) because the plot shows $\dot{\boldsymbol{r}}_{B/N}$ and not $\dot{\boldsymbol{r}}_{C/N}$, the latter of which would not oscillate. As for the angular velocity, the oscillations are due to the natural gyroscopic terms from Euler's equation $[I]\dot{\boldsymbol{\omega}} = -\boldsymbol{\omega} \times ([I]\boldsymbol{\omega})$.

In the second simulation, instead of having two bodies connected by 1-DoF joints, only one component is connected through a 2-DoF joint. This simulation shares the same equations and implementation as the first simulation. The only differences lie in how the module is set up. This configuration, where a single panel is connected to the rigid hub, is shown in Fig. 9. The panel consists of a flat disk with a diameter of 2 m and a thickness of 0.1 m. It is attached to the hub through a universal joint (2 degrees of freedom). The subsystem's properties are shown in Table 5. Since the joint has 2 degrees of freedom, the lower body's mass and inertia are zero.

The time history for both θ angles and $\dot{\theta}$ angle rates is given in Figs. 10a and 10b. The response differs from the one in seven. The angles and angle rates settle much faster because there is no cross-coupling between two rigid bodies, although the response still resembles a spring-damper system.

The time history for the hub's velocity and angular velocity are given in Figs. 11a and 11b. Again, two distinct phases are evident: the initial transient and the steady-state behavior. Note that since the angles damp out quicker in this scenario, the transient behavior is also

[¶¶]Data available online at https://hanspeterschaub.info/basilisk.

[***]Data available online at https://hanspeterschaub.info/basilisk/examples/scenarioSpinningBodiesTwoDOF.html.

Table 4 Simulation parameters for the two-panel simulation

Parameter	Notation	Value	Units
Panel 1's mass	m_{S_1}	20	kg
Panel 2's mass	m_{S_2}	20	kg
Panel 1's inertia about its center of mass	${}^{\mathcal{S}_1}[I_{S_1,S_{c_1}}]$	${}^{\mathcal{S}_1}\begin{bmatrix} 26.7(3) & 0 & 0 \\ 0 & 6.7(3) & 0 \\ 0 & 0 & 33.(3) \end{bmatrix}$	kg · m^2
Panel 2's inertia about its center of mass	${}^{\mathcal{S}_2}[I_{S_2,S_{c_2}}]$	${}^{\mathcal{S}_2}\begin{bmatrix} 26.7(3) & 0 & 0 \\ 0 & 6.7(3) & 0 \\ 0 & 0 & 33.(3) \end{bmatrix}$	kg · m^2
Panel 1's center-of-mass location with respect to S_1	${}^{\mathcal{S}_1}\boldsymbol{r}_{S_{c_1}/S_1}$	${}^{\mathcal{S}_1}[0, 2, 0]^T$	m
Panel 2's center-of-mass location with respect to S_2	${}^{\mathcal{S}_2}\boldsymbol{r}_{S_{c_2}/S_2}$	${}^{\mathcal{S}_2}[0, 2, 0]^T$	m
Position of the origin of the S_1 frame relative to B	${}^{\mathcal{B}}\boldsymbol{r}_{S_1/B}$	${}^{\mathcal{B}}[0, 1, 0.95]^T$	m
Position of the origin of the S_2 frame relative to S_1	${}^{\mathcal{S}_1}\boldsymbol{r}_{S_2/S_1}$	${}^{\mathcal{S}_1}[-1, 2, 0]^T$	m
DCM of the S_1 equilibrium frame with respect to the B frame	${}^{\mathcal{B}}[S_{01}B]$	${}^{\mathcal{B}}\begin{bmatrix} 1 & 0 & 0 \\ 0 & 1 & 0 \\ 0 & 0 & 1 \end{bmatrix}$	— —
DCM of the S_2 equilibrium frame with respect to the S_1 frame	${}^{\mathcal{S}_1}[S_{02}S_1]$	${}^{\mathcal{S}_1}\begin{bmatrix} 1 & 0 & 0 \\ 0 & 1 & 0 \\ 0 & 0 & 1 \end{bmatrix}$	— —
Rotation axis for S_1	${}^{\mathcal{B}}\hat{s}_1$	${}^{\mathcal{B}}[1, 0, 0]^T$	— —
Rotation axis for S_2	${}^{\mathcal{S}_1}\hat{s}_2$	${}^{\mathcal{S}_1}[0, 1, 0]^T$	— —
Torsional linear spring constant for $\hat{s}_1$	k_1	50	N · m/rad
Torsional linear spring constant for $\hat{s}_2$	k_2	50	N · m/rad
Torsional linear damper constant for $\hat{s}_1$	c_1	30	N · m/rad
Torsional linear damper constant for $\hat{s}_2$	c_2	30	N · m/rad

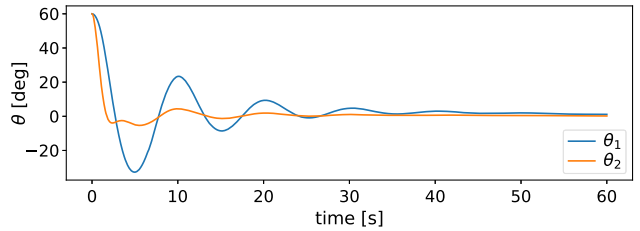

a) Angles for each hinged panel

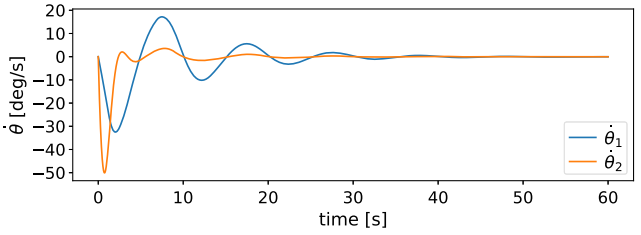

b) Angle rates for each hinged panel

Fig. 7 Time history for component states using two panels.

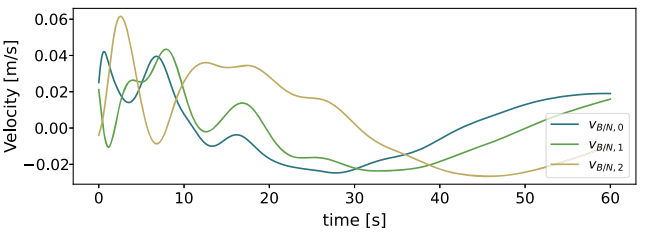

a) Velocity of the hub

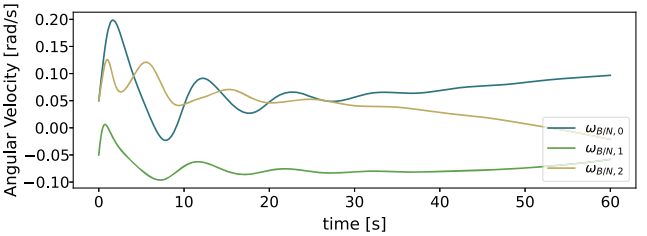

b) Angular velocity of the hub

Fig. 8 Time history for the hub's states using two panels.

shorter than in the two-panel simulation. This is another clear effect of the coupling between the panel and the hub that is evident in the equations of motion.

VI. Conclusions

As spacecraft become more complex, there is a need for robust simulation architectures that can replicate the spacecraft's behavior throughout its mission. Creating a general and modular representation of common categories of spacecraft components saves time and effort for the engineers while retaining the high fidelity needed to guarantee that the mission objectives are met. This work provides an architecture and the corresponding equations of motion for simulating single and dual-axis rotating rigid components in a general, modular way.

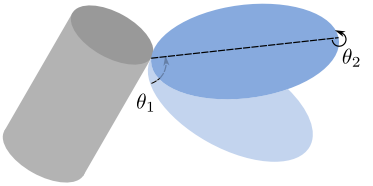

Fig. 9 Spacecraft with a hub and a panel connected through a universal joint.

A dynamics architecture is proposed, where shared component structures are created to minimize repeating equations of motion and centralize the verification of common properties attributes. The equations of motion of the single and dual-axis effectors are comprehensively derived without making any assumptions on the

Table 5 Simulation parameters for the single-panel simulation

Parameter	Notation	Value	Units
Panel 1's mass	m_{S_1}	0	kg
Panel 2's mass	m_{S_2}	50	kg
Panel 1's inertia about its center of mass	${}^{\mathcal{S}_1}[I_{S_1,S_{c_1}}]$	${}^{\mathcal{S}_1}\begin{bmatrix} 0 & 0 & 0 \\ 0 & 0 & 0 \\ 0 & 0 & 0 \end{bmatrix}$	kg · m^2
Panel 2's inertia about its center of mass	${}^{\mathcal{S}_2}[I_{S_2,S_{c_2}}]$	${}^{\mathcal{S}_2}\begin{bmatrix} 50.041(6) & 0 & 0 \\ 0 & 50.041(6) & 0 \\ 0 & 0 & 100 \end{bmatrix}$	kg · m^2
Panel 1's center-of-mass location with respect to S_1	${}^{\mathcal{S}_1}\boldsymbol{r}_{S_{c_1}/S_1}$	${}^{\mathcal{S}_1}[0,0,0]^T$	m
Panel 2's center-of-mass location with respect to S_2	${}^{\mathcal{S}_2}\boldsymbol{r}_{S_{c_2}/S_2}$	${}^{\mathcal{S}_2}[0,2,0]^T$	m
Position of the origin of the S_1 frame relative to B	${}^{\mathcal{B}}\boldsymbol{r}_{S_1/B}$	${}^{\mathcal{B}}[0,1,0.95]^T$	m
Position of the origin of the S_2 frame relative to S_1	${}^{\mathcal{S}_1}\boldsymbol{r}_{S_2/S_1}$	${}^{\mathcal{S}_1}[0,0,0]^T$	m
DCM of the S_1 equilibrium frame with respect to the B frame	${}^{\mathcal{B}}[S_{01}B]$	${}^{\mathcal{B}}\begin{bmatrix} 1 & 0 & 0 \\ 0 & 1 & 0 \\ 0 & 0 & 1 \end{bmatrix}$	— —
DCM of the S_2 equilibrium frame with respect to the S_1 frame	${}^{\mathcal{S}_1}[S_{02}S_1]$	${}^{\mathcal{S}_1}\begin{bmatrix} 1 & 0 & 0 \\ 0 & 1 & 0 \\ 0 & 0 & 1 \end{bmatrix}$	— —
Rotation axis for S_1	${}^{\mathcal{B}}\hat{s}_1$	${}^{\mathcal{B}}[1,0,0]^T$	— —
Rotation axis for S_2	${}^{\mathcal{S}_1}\hat{s}_2$	${}^{\mathcal{S}_1}[0,1,0]^T$	— —
Torsional linear spring constant for $\hat{s}_1$	k_1	100	N · m/rad
Torsional linear spring constant for $\hat{s}_2$	k_2	100	N · m/rad
Torsional linear damper constant for $\hat{s}_1$	c_1	50	N · m/rad
Torsional linear damper constant for $\hat{s}_2$	c_2	50	N · m/rad

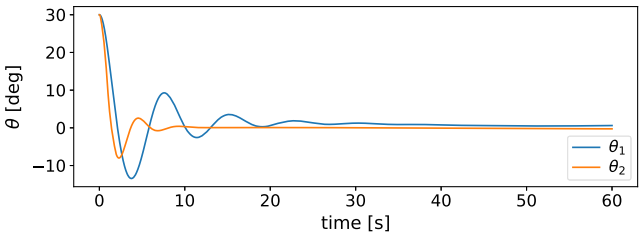

a) Angles for each hinge

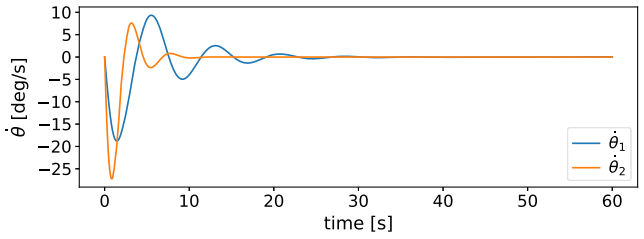

b) Angle rates for each hinge

Fig. 10 Time history for component states using one panel.

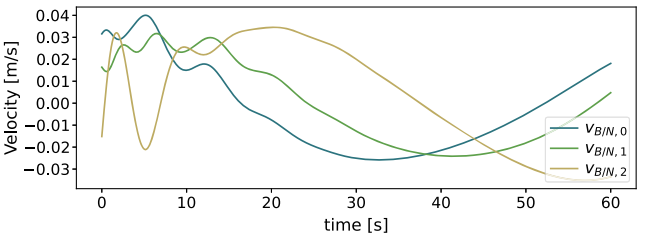

a) Velocity of the hub

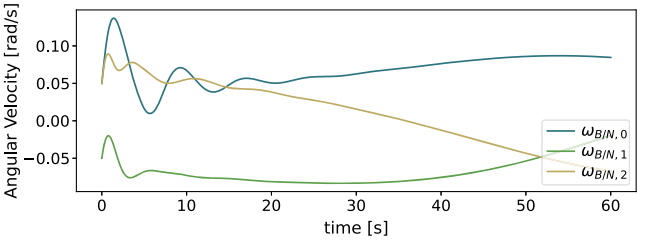

b) Angular velocity of the hub

Fig. 11 Time history for the hub's states using two panels.

frame, spin axis, or the location of the center of mass. The outcome is a universal formulation of the equations that describe these components. Verification is completed for both formulations by verifying energy and angular momentum conservation, which is shown in the Appendix. It is shown that both models agree to these fundamental physical conservation laws when only conservative forces are present.

Appendix: Verification of the Equations of Motion in Software

Verification is a crucial step in implementing the equations of motion. It is impossible to guarantee that the equations are correct and implemented appropriately without verifying the approach. In addition, the verified method verifies that some conservation laws are respected by checking whether some physical quantities remain constant throughout the simulation. While this alone does not guarantee that the equations are correct, it gives high confidence that they have been correctly derived and implemented.

The quantities being verified are the orbital energy, the orbital angular momentum, the rotational energy, and the rotational angular momentum. In the presence of gravity, a conservative force, energy should be constant. Moreover, since gravity is a radial force, the orbital angular momentum is also constant throughout the simulation. The rotational quantities should also remain constant without torques and nonconservative forces. The complete derivation and explanation of why these quantities must be conserved are given in Ref. [6].

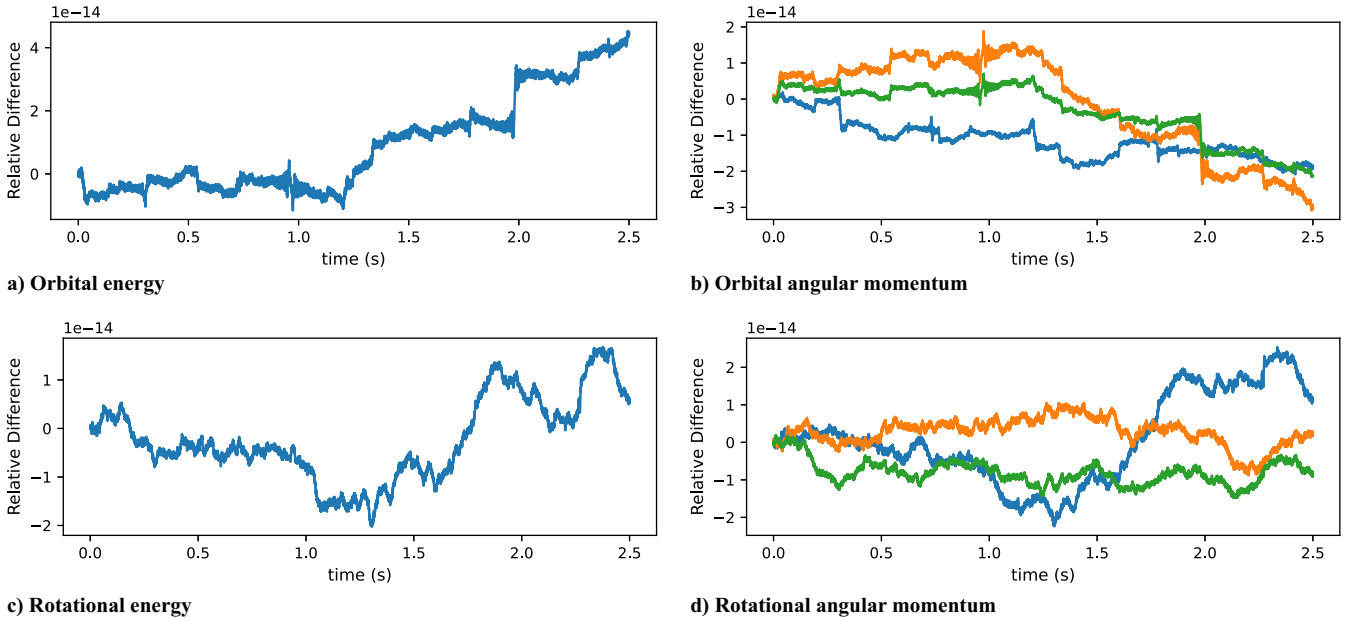

a) Orbital energy

b) Orbital angular momentum

c) Rotational energy

d) Rotational angular momentum

Fig. A1 Verification for the single-axis component module.

A. Single-Axis Rotating Rigid Body

The verification results are given in Figs. A1a–A1d. It should be noted that while the plots do not immediately look constant, the scale on the vertical axis is on the order of 10^{-15} to 10^{-14}. This is very close to machine precision, which means numerical errors slightly corrupt the data. Moreover, the random walk in these plots is very common in fixed-step integrators like the fourth-order Runge–Kutta used in these simulations.

B. Dual-Axis Rotating Rigid-Body Dynamics

The same verification tests are performed for the dual-axis rotating rigid-body system, shown in Figs. B1a–B1d. As before, the angular momentum and energy quantities are conserved throughout the simulation, as only conservative forces and torques are acting on the spacecraft. This implies a high confidence level that both the mathematical derivation and the software implementation are correct and follow fundamental physical principles.

Acknowledgments

Cody Allard would like to acknowledge Joel Runnels and Jesse Keefer from Ball Aerospace. Joel Runnels for his object-oriented brilliance and ability to abstract a dynamics problem into objects, and Jesse Keefer for working together on related projects to this work.

References

[1] Gibb, J., "Lightweight Flexible Space Solar Arrays, Past, Present and Future," *2018 IEEE 7th World Conference on Photovoltaic Energy Conversion (WCPEC) (A Joint Conference of 45th IEEE PVSC, 28th PVSEC & 34th EU PVSEC)*, IEEE Publ., Piscataway, NJ, 2018, pp. 3530–3534. https://doi.org/10.1109/PVSC.2018.8547918

[2] Sovey, J. S., Rawlin, V. K., and Patterson, M. J., "Ion Propulsion Development Projects in US: Space Electric Rocket Test I to Deep Space 1," *Journal of Propulsion and Power*, Vol. 17, No. 3, 2001, pp. 517–526.

[3] Brophy, J. R., "NASA's Deep Space 1 Ion Engine (Plenary)," *Review of Scientific Instruments*, Vol. 73, No. 2, 2002, pp. 1071–1078.

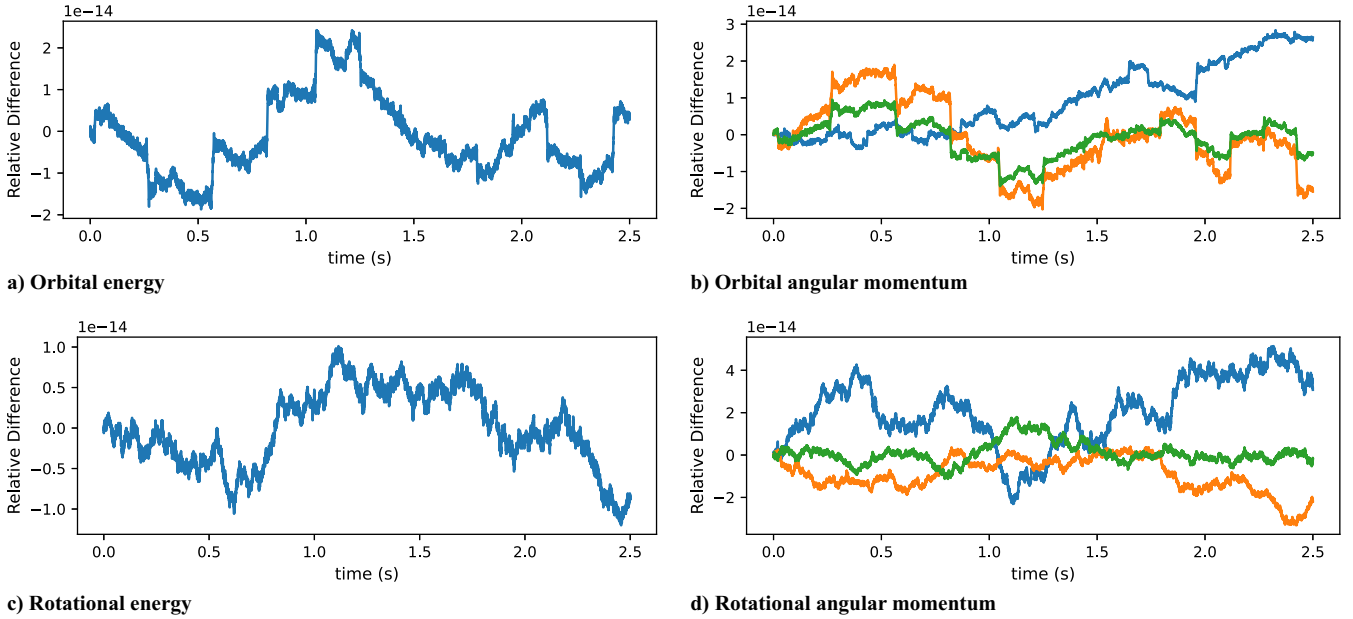

a) Orbital energy

b) Orbital angular momentum

c) Rotational energy

d) Rotational angular momentum

Fig. B1 Verification for the dual-axis component module.

[4] Brophy, J., Garner, C., Nakazono, B., Marcucci, M., Henry, M., and Noon, D., "The Ion Propulsion System for Dawn," *39th AIAA/ASME/SAE/ASEE Joint Propulsion Conference and Exhibit*, AIAA Paper 2003-4542, 2003.

[5] Oh, D. Y., Collins, S., Drain, T., Hart, W., Imken, T., Larson, K., Marsh, D., Muthulingam, D., Snyder, J. S., Trofimov, D., et al., "Development of the Psyche Mission for NASA's Discovery Program," *36th International Electric Propulsion Conference*, Univ. of Vienna Paper IEPC-2019-192, Sept. 2019.

[6] Allard, C., Diaz-Ramos, M., Kenneally, P. W., Schaub, H., and Piggott, S., "Modular Software Architecture for Fully-Coupled Spacecraft Simulations," *Journal of Aerospace Information Systems*, Vol. 15, No. 12, 2018, pp. 670–683. https://doi.org/10.2514/1.I010653

[7] Allard, C., Diaz-Ramos, M., and Schaub, H., "Computational Performance of Complex Spacecraft Simulations Using Back-Substitution," *Journal of Aerospace Information Systems*, Vol. 16, No. 10, 2019, pp. 427–436. https://doi.org/10.2514/1.I010713

[8] Alcorn, J., Allard, C., and Schaub, H., "Fully Coupled Reaction Wheel Static and Dynamic Imbalance for Spacecraft Jitter Modeling," *Journal of Guidance, Control, and Dynamics*, Vol. 41, No. 6, 2018, pp. 1380–1388. https://doi.org/10.2514/1.G003277

[9] Alcorn, J., Allard, C., and Schaub, H., "Fully-Coupled Dynamical Jitter Modeling of Variable-Speed Control Moment Gyroscopes," *AAS/AIAA Astrodynamics Specialist Conference*, AAS Paper 17-730, 2017.

[10] Allard, C., Schaub, H., and Piggott, S., "General Hinged Solar Panel Dynamics Approximating First-Order Spacecraft Flexing," *Journal of Spacecraft and Rockets*, Vol. 55, No. 5, 2018, pp. 1290–1298. https://doi.org/10.2514/1.A34125

[11] Panicucci, P., Allard, C., and Schaub, H., "Spacecraft Dynamics Employing a General Multi-Tank and Multi-Thruster Mass Depletion Formulation," *Journal of Astronautical Sciences*, Vol. 65, No. 4, 2018, pp. 423–447. https://doi.org/10.1007/s40295-018-0133-0

[12] Allard, C., Maxwell, J., and Schaub, H., "A Transport Theorem for the Inertia Tensor for Simplified Spacecraft Dynamics Development," *International Astronautical Congress*, International Astronautical Federation, Paris, France, 2022.

[13] Schaub, H., and Junkins, J. L., *Analytical Mechanics of Space Systems*, 4th ed., AIAA Education Series, AIAA, Reston, VA, 2018, Chaps. 1, 2, 4. https://doi.org/10.2514/4.105210

[14] Bercovici, B., Amirkaveh, C., Vindry, G., and Masset, A., "Automated GNC FSW Integration and Testing Using the Basilisk Framework," *AAS Guidance and Control Conference*, AAS Paper 23-081, 2023.

[15] Kramlich, R., Huun, J., Garcia, A., Cohen, A., and Gaston, T., "Validation of the Guidance, Navigation, and Control (GNC) Architecture for RPO Missions Using Basilisk-cFS Architecture," *AAS/AIAA Astrodynamics Specialist Conference*, AAS Paper 23-161, 2023.

[16] Vaz Carneiro, J., Allard, C., and Schaub, H., "Rotating Rigid Body Dynamics Architecture For Spacecraft Simulation Software Implementation," *AAS Guidance and Control Conference*, AAS Paper 23-112, 2023.

[17] Kenneally, P. W., Piggott, S., and Schaub, H., "Basilisk: A Flexible, Scalable and Modular Astrodynamics Simulation Framework," *Journal of Aerospace Information Systems*, Vol. 17, No. 9, 2020, pp. 496–507. https://doi.org/10.2514/1.I010762

[18] Géradin, M., and Rixen, D. J., *Mechanical Vibrations: Theory and Application to Structural Dynamics*, Wiley, New York, 2014, Chap. 1.

[19] Kane, T. R., and Levinson, D. A., *Dynamics, Theory and Applications*, McGraw–Hill, New York, 1985, Chap. 4.

[20] Roithmayr, C. M., and Hodges, D. H., "Dynamics: Theory and Application of Kane's Method," *Journal of Computational and Nonlinear Dynamics*, Vol. 11, No. 6, 2016, Paper 066501.

[21] Rodriguez, G., Jain, A., and Kreutz-Delgado, K., "A Spatial Operator Algebra for Manipulator Modeling and Control," *International Journal of Robotics Research*, Vol. 10, No. 4, 1991, pp. 371–381. https://doi.org/10.1177/027836499101000406

[22] Rodriguez, G., Jain, A., and Kreutz, K., "Spatial Operator Algebra Framework for Multibody System Dynamics," *Journal of the Astronautical Sciences*, Vol. 40, No. 1, 1992, pp. 27–50.

[23] Jain, A., and Rodriguez, G., "Recursive Flexible Multibody Dynamics Using Spatial Operators," *Advances in Factories of the Future, CIM and Robotics, Manufacturing Research and Technology*, Vol. 16, edited by M. Cotsaftis, and F. Vernadat, Elsevier, New York, 1993, pp. 345–358, https://www.sciencedirect.com/science/article/pii/B9780444898562500363. https://doi.org/10.1016/B978-0-444-89856-2.50036-3

V. Babuska
Associate Editor